Supporting Information (SI)

Molecular engineering by triptycene groups enables homoleptic Ir(III) complexes with enhanced electroluminescent properties

Zheng-Yu Tao,[†a] Ze-Hui Pan,[†b] Ying-Jie Wang,[†a] Jialing Zhang,[a] Qing-Song Wang,[a] Qian-Feng Zhang,[a] Bi-Hai Tong,*[a] Man-Keung Fung,*[b] and Hui Kong*[a]

[a]Key Laboratory of Metallurgical Emission Reduction & Resources Recycling, Ministry of Education, Institute of Molecular Engineering and Applied Chemistry, School of Metallurgy Engineering, Anhui University of Technology, Maanshan, 243002, Anhui, China. E-mail: tongbihai@ahut.edu.cn, konghui@ahut.edu.cn

[b]Jiangsu Key Laboratory for Carbon-Based Functional Materials & Devices, Institute of Functional Nano & Soft Materials (FUNSOM) & Collaborative Innovation Center of Suzhou Nano Science and Technology, Soochow University, Suzhou 215123, P. R. China. E-mail: mkfung@suda.edu.cn

[†] Authors contributed equally.

Contents:

1. General descriptions
2. X-ray crystal structure data
3. Photophysical data
4. Reference device data
5. ^{1}H- and ^{19}F-NMR spectra and high resolution mass spectrometers (HRMS) of all new compounds
6. References

1. General descriptions

1.1. Materials and characterization

All the materials and solvents were obtained commercially and used as received without further purification. Proton NMR spectra were measured on a Bruker AV400 spectrometer. High resolution mass spectra (HRMS) were recorded with a TOF 5600^{plus} mass spectrometer. X-ray crystallography diffraction was carried out on a Bruker SMART Apex CCD diffractometer. Cyclic voltammetry (CV) was measured on a CHI1140B Electrochemical Analyzer through a three-electrode system with a glassy carbon disk as the working electrode, platinum plate as the counter electrode and Ag/AgCl as the reference electrode. UV/Vis absorption spectra were recorded on a Purkinje General TU-1901 spectrophotometer. The PL spectra were recorded on a PerkinElmer LS-55 fluorescence spectrophotometer. The PL quantum efficiency and lifetime were measured with an Edinburgh FLS980 instrument.

1.2. Computational methodology

B3LYP functional was used to optimize the geometrical structures of ground state (S_0).[1] A "double-ξ" quality basis set consisting of Hay and Wadt's effective core potentials (ECP), LANL2DZ,[2] was employed to the Ir atom. 6-31G(d) basis set[3] was applied to other nonmetallic atoms. The solvent effect in CH_2Cl_2 medium was considered throughout the calculations. Combined with VMD program,[5] the molecular orbital was visualized by Multiwfn code.[4] The frontier molecular orbital (FMO) distribution in molecules was analyzed by Multiwfn using Mulliken population analysis. Gaussian 16 software package was used for calculations.[6]

1.3. OLED fabrication

The OLEDs were grown on pre-patterned ITO coated glass (≈ 20 Ω square^{-1}). Before depositing into the evaporation system, the ITO substrates were cleaned with acetone, ethyl alcohol, and deionized water by ultrasonic cleaning machine for 20 min. All the devices were deposited sequentially under fine vacuum of 8×10^{-5} Pa. The organic transport materials were grown by the rate of 0.08-0.15 nm s^{-1}, while organic dopants, AlQ_3 were deposited at the rate of 0.02-0.15 Å s^{-1}, Al was deposited by the rate of 3 Å s^{-1}. The CIE coordinates, luminance, and EL spectra were carried out by a PR655 spectra-scan photometer simultaneously. The current density-voltage

characteristics were tested by a programmable Keithley source-measure 2400 and PR655 spectra-scan.

1.4. Synthetic routes of key intermediates

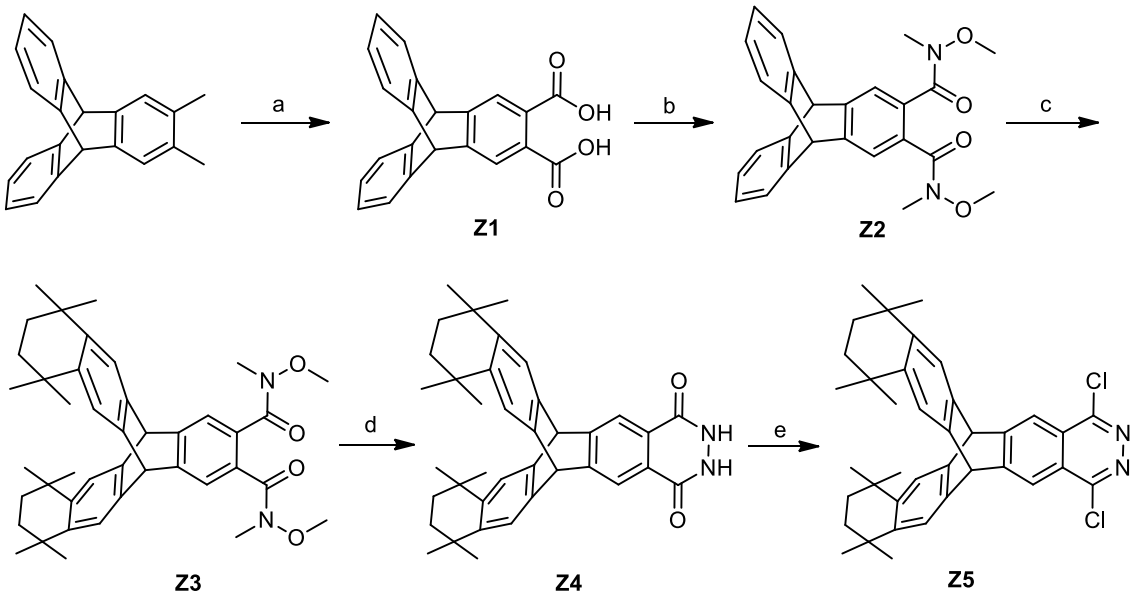

Scheme S1 Synthetic routes of key intermediates: a) $KMnO_4$, pyridine/H_2O, reflux, 12 h; b) NHMe(OMe), PCl_3, 60 ℃, 1.5 h; c) 2,5-dichloto-2,5-dimethylhexane, $AlCl_3$, CH_2Cl_2, 0 ℃, 2 h; d) hydrazine hydrate (98%), ethanol, reflux, 12 h; e) $POCl_3$, reflux, 12 h.

Triptycene-2,3-dicarboxylic acid (Z1):

$KMnO_4$ (22.5 g, 140 mmol) was added in batches over 12 h to a refluxing solution of 2,3-dimethyltriptycene (2.0 g, 7 mmol, prepared by 2,3-dimethylanthracene and anthranilic acid according to the literature method[1]) in a mixture of pyridine (20 mL) and H_2O (40 mL). Then, the precipitate was filtered off and washed with 1% aqueous solution of NaOH. The filtrate was acidified to pH 1 with dilute hydrochloric acid. The precipitated product was collected by filtration and dried as white powder (2.2 g, 91%). ^{1}H NMR (400 MHz, DMSO-*d6*) δ 13.10 (br, 2 H), 7.77 (s, 2 H), 7.50 – 7.42 (m, 4 H), 7.06 – 6.98 (m, 4 H), 5.82 (s, 2 H).

N^2, N^3-Dimethoxy-N^2,N^3-dimethyl-triptycene-2,3-dicarboxamide (Z2):

A solution of NHMe(OMe) (3.6 g, 60.0 mmol) and triptycene-2,3-dicarboxylic acid (1.0 g, 2.9 mmol) was stirred in dry toluene (20 mL) at 0 °C for 10 min. PCl_3 (1.2 g, 8.7 mmol) was then added dropwise to the mixture. The mixture was warmed to r.t. slowly and then stirred at 60 °C for 1.5 h. Then the mixture was cooled to r.t. and quenched with saturated $NaHCO_3$ aqueous solution and

extracted with EtOAc. The combined organic layers were dried and the solvent was removed in vacuo. The pure product was obtained as white powder (1.3 g, 83%). ^{1}H NMR (400 MHz, DMSO-*d6*) δ 7.57 (s, 2 H), 7.49 – 7.45 (M, 4 H), 7.05 – 7.01 (m, 4 H), 5.78 (s, 2 H), 3.46 (s, 6 H), 3.12 (s, 6 H).

N^{18},N^{19}-Dimethoxy-N^{18},N^{19},1,1,4,4,8,8,11,11-decamethyl-1,2,3,4,6,8,9,10,11,13-decahydro-6,13-[1,2]benzenopentacene-18,19-dicarboxamide (Z3):

A solution of **Z2** (0.5 g, 1.2 mmol), 2,5-dichloto-2,5-dimethylhexane (0.7 g 3.6 mmol) and $AlCl_3$ (0.8 g, 6 mmol) in CH_2Cl_2 (15 mL) was stirred at 0 ℃ for 2 h. Then the mixture was quenched with H_2O and extracted with CH_2Cl_2. The combined organic layers were washed with ammonia and dried. The solvent was removed in vacuo. The residue was purified by column chromatography on silica gel using petroleum ether/ethyl acetate (V:V=3:2) as the eluent to yield **Z3** (0.45 g, 60%) as a white solid. ^{1}H NMR (400 MHz, $CDCl_3$) δ 7.45 (s, 2 H), 7.27 (s, 4 H), 5.28 (s, 2 H), 3.58 (s, 6 H), 3.25 (s, 6H), 1.61 (s, 8 H), 1.22 (s, 24 H).

1,1,4,4,8,8,11,11-Octamethyl-1,2,3,4,8,9,10,11,18,19-decahydro-6,13-[6,7]epiphthalazinopentacene-17,20(6H,13H)-dione (Z4):

A solution of **Z3** (2.0 g, 3 mmol) and hydrazine hydrate (98%, 3 mL) in ethanol (20 mL) was refluxed for 12 h under N_2 atmosphere. Then the solvent was removed in vacuo. The residue was purified by column chromatography on silica gel using petroleum ether/ethyl acetate (V:V=3:2) as the eluent to yield **Z4** (1.5 g, 87%) as a white solid. ^{1}H NMR (400 MHz, $CDCl_3$) δ 8.19 (s, 2 H), 7.34 (s, 4 H), 5.51 (s, 2 H), 1.59 (s, 8 H), 1.24 (s, 24 H).

17,20-Dichloro-1,1,4,4,8,8,11,11-octamethyl-1,2,3,4,6,8,9,10,11,13-decahydro-6,13-[6,7]epiphthalazinopentacene (Z5):

A solution of **Z4** (0.85 g, 2.5 mmol) in $POCl_3$ (7 mL) was refluxed for 12 h under N_2 atmosphere. The mixture was cooled to r.t. and poured into ice water. The mixture was adjusted to weakly alkaline with $NaHCO_3$ and extracted with CH_2Cl_2. The combined organic layers were washed with ammonia and dried. The residue was purified by flash column chromatography on silica gel using CH_2Cl_2 as the eluent to yield **Z5** (0.55 g, 61%) as a white solid. Because this product was sensitive to water, it was not further purified and the next reaction was directly carried out.

2. X-ray crystal structure data

Table S1 Crystallographic refinement data of complexes **Ir1**, **Ir2** and **Ir3**.

Compound	**Ir1**	**Ir2**	**Ir3**
Empirical formula	$C_{96}H_{51}F_{18}Ir\ N_6$	$C_{108}H_{57}F_{18}IrN_6$	$C_{108}H_{57}F_{18}IrN_6$
Formula weight	1822.62	1972.79	1972.79
Temperature	296(2) K	296(2) K	296(2) K
Wavelength	0.71073 Å	0.71073 Å	0.71073 Å
Crystal system	Triclinic	Trigonal	Monoclinic
Space group	*P-1*	R-3	$P2_1/c$
Unit cell dimensions	a = 15.821(6) Å α = 73.051(5)°	a = 23.222(6) Å α = 90°	a = 15.492(4) Å α = 90°
	b = 16.604(7) Å β = 79.335(5)°	b = 23.222(6) Å β = 90°	b = 23.882(6) Å β = 94.240(5)°
	c = 16.741(7) Å γ = 78.608(5)°	c = 36.092(9) Å γ = 120°	c = 27.611(7) Å γ = 90°
Volume	4085.5(3) $Å^3$	16856(9) $Å^3$	10188(4) $Å^3$
Z	2	6	4
Density (calculated)	1.482 Mg/m^3	1.166 Mg/m^3	1.286 Mg/m^3
Absorption coefficient	1.727 mm^{-1}	1.261 mm^{-1}	1.391 mm^{-1}
F(000)	1816	5916	3944
Crystal size	0.22 x 0.2 x 0.18 mm^3	0.260 x 0.240 x 0.200 mm^3	0.250 x 0.200 x 0.180 mm^3
Theta range for data collection	2.279 to 24.999°	2.102 to 24.996°	2.053 to 25.000°
Index ranges	-18<=h<=18, -18<=k<=19, -16<=l<=19	-27<=h<=18, -27<=k<=27, -37<=l<=42	-18<=h<=18, -28<=k<=20, -32<=l<=32
Reflections collected	20932	29068	53030
Independent reflections	14062 [R(int) = 0.0382]	6586 [R(int) = 0.0314]	17865 [R(int) = 0.1454]
Completeness to theta = 25.000°	97.7 %	99.7 %	99.5 %
Absorption correction	Semi-empirical from equivalents	Semi-empirical from equivalents	Semi-empirical from equivalents
Max. and min. transmission	0.746 and 0.702	0.787 and 0.735	0.788 and 0.722
Refinement method	Full-matrix least-squares on F^2	Full-matrix least-squares on F^2	Full-matrix least-squares on F^2
Data / restraints / parameters	14062 / 1234 / 1090	6586 / 480 / 400	17865 / 1392 / 1198
Goodness-of-fit on F^2	0.947	0.894	0.940
Final R indices [I>2sigma(I)]	R1 = 0.0488, wR2 = 0.1296	R1 = 0.0339, wR2 = 0.0966	R1 = 0.0641, wR2 = 0.1078
R indices (all data)	R1 = 0.0770, wR2 = 0.1458	R1 = 0.0404, wR2 = 0.1007	R1 = 0.1454, wR2 = 0.1281
Extinction coefficient	n/a	n/a	n/a
Largest diff. peak and hole	1.627 and -1.200 $e.Å^{-3}$	0.968 and -0.626 $e.Å^{-3}$	1.300 and -0.991 $e.Å^{-3}$

Table S2 Selected bond lengths [Å] and angles [°] for complexes **Ir1**, **Ir2** and **Ir3**.

Ir1		**Ir2**		**Ir3**	
Ir(1)-C(2)	2.016(5)	Ir(01)-C(5)#1	2.017(3)	Ir(01)-C(2)	2.001(6)
Ir(1)-C(81)	2.016(6)	Ir(01)-C(5)#2	2.017(3)	Ir(01)-C(68)	2.004(7)
Ir(1)-C(33)	2.038(6)	Ir(01)-C(5)	2.017(3)	Ir(01)-C(102)	2.026(7)
Ir(1)-N(5)	2.101(5)	Ir(01)-N(2)#1	2.089(2)	Ir(01)-N(5)	2.077(5)
Ir(1)-N(1)	2.112(5)	Ir(01)-N(2)#2	2.089(2)	Ir(01)-N(3)	2.091(6)
Ir(1)-N(3)	2.113(5)	Ir(01)-N(2)	2.089(2)	Ir(01)-N(1)	2.102(5)
C(2)-Ir(1)-C(81)	92.4(2)	C(5)#1-Ir(01)-C(5)#2	96.99(10)	C(2)-Ir(01)-C(68)	96.4(3)
C(2)-Ir(1)-C(33)	96.3(2)	C(5)#1-Ir(01)-C(5)	96.98(10)	C(2)-Ir(01)-C(102)	96.9(3)
C(81)-Ir(1)-C(33)	98.6(2)	C(5)#2-Ir(01)-C(5)	96.98(10)	C(68)-Ir(01)-C(102)	93.7(3)
C(2)-Ir(1)-N(5)	90.3(2)	C(5)#1-Ir(01)-N(2)#1	78.27(11)	C(2)-Ir(01)-N(5)	79.2(3)
C(81)-Ir(1)-N(5)	79.2(2)	C(5)#2-Ir(01)-N(2)#1	91.19(10)	C(68)-Ir(01)-N(5)	169.7(3)
C(33)-Ir(1)-N(5)	173.17(19)	C(5)-Ir(01)-N(2)#1	171.02(10)	C(102)-Ir(01)-N(5)	96.1(2)
C(2)-Ir(1)-N(1)	78.9(2)	C(5)#1-Ir(01)-N(2)#2	171.02(10)	C(2)-Ir(01)-N(3)	93.9(3)
C(81)-Ir(1)-N(1)	168.99(19)	C(5)#2-Ir(01)-N(2)#2	78.26(11)	C(68)-Ir(01)-N(3)	78.9(3)
C(33)-Ir(1)-N(1)	89.1(2)	C(5)-Ir(01)-N(2)#2	91.19(10)	C(102)-Ir(01)-N(3)	167.5(3)
N(5)-Ir(1)-N(1)	93.94(18)	N(2)#1-Ir(01)-N(2)#2	94.11(9)	N(5)-Ir(01)-N(3)	92.0(2)
C(2)-Ir(1)-N(3)	175.22(19)	C(5)#1-Ir(01)-N(2)	91.19(10)	C(2)-Ir(01)-N(1)	168.9(2)
C(81)-Ir(1)-N(3)	89.3(2)	C(5)#2-Ir(01)-N(2)	171.02(10)	C(68)-Ir(01)-N(1)	94.2(2)
C(33)-Ir(1)-N(3)	79.0(2)	C(5)-Ir(01)-N(2)	78.26(11)	C(102)-Ir(01)-N(1)	79.1(3)
N(5)-Ir(1)-N(3)	94.44(18)	N(2)#1-Ir(01)-N(2)	94.11(9)	N(5)-Ir(01)-N(1)	90.9(2)
N(1)-Ir(1)-N(3)	99.92(18)	N(2)#2-Ir(01)-N(2)	94.11(9)	N(3)-Ir(01)-N(1)	91.4(2)

3. Photophysical data

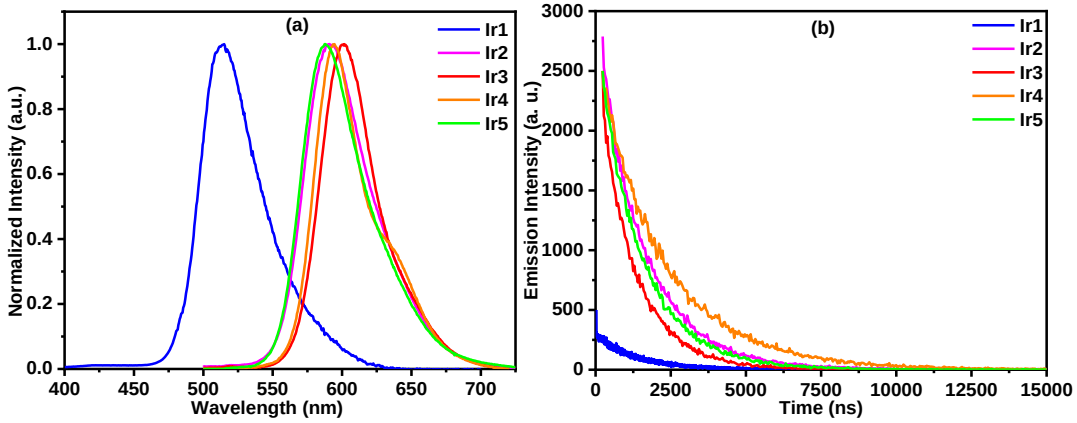

Fig. S1 PL spectra of new iridium complex in PMMA films at a conc. of 1 wt% (a) and the emission decay curves (b) at RT.

4. Reference device data

The doping concentration of the reference emitter **PO-01** was 10 wt%, corresponding to reference device **C**.

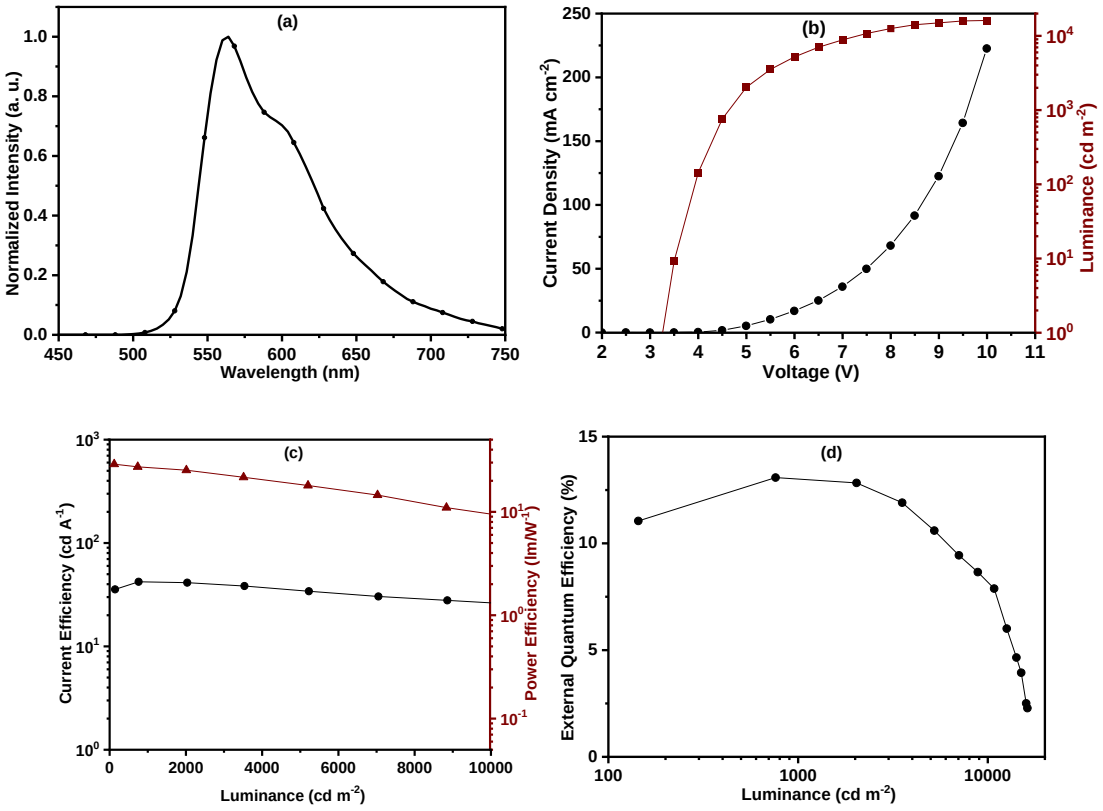

Fig. S2 (a) Electroluminescence spectrum of the reference device. (b) The luminance-voltage characteristic of reference device. (c) The current efficiency-luminance-power efficiency characteristic of reference device. (d) The EQE characteristic of reference device.

Table S3 Summary of reference device luminescence and efficiency data.

Device (dopant)	λ_{EL}[a] (nm)	V_{on}[b] (V)	L[c] (cd m^{-2})	CE[d] (cd A^{-1})	PE[d] (lm W^{-1})	EQE[d] (%)	CIE[a] (x, y)
C (**PO-01**)	564	3.2	16170	42.1 (42.0)	29.0 (26.9)	13.1 (13.0)	(0.50,0.49)

(a) Values at 7 V; (b) Turn on voltages at 1 cd m^{-2}; (c) Maximum luminance; (d) Maximum efficiency (efficiency at 1000 cd m^{-2}).

Table S4 Concentration optimization experimental device luminescence and efficiency data.

Sample (concentration)	λ_{EL}[a] (nm)	V_{on}[b] (V)	L[c] (cd m^{-2})	CE[d] (cd A^{-1})	PE[d] (lm W^{-1})	EQE[d] (%)
Ir1 (10 wt%)	524	3.2	18410	46.3	45.5	15.8
Ir1 (15 wt%)	526	3.1	24510	48.5	47.6	17.1
Ir1 (20 wt%)	526	3.2	22190	44.1	43.3	14.9
Ir2 (2 wt%)	588	3.8	15190	46.4	38.3	27.3
Ir2 (3 wt%)	592	4.0	19067	46.4	35.64	27.5
Ir2 (4 wt%)	592	3.8	19870	44.6	35.18	26.5
Ir2 (5 wt%)	596	3.8	15251	40.1	28.5	23.8

(a) Values at 6 V; (b) Turn on voltages at 1 cd m^{-2}; (c) Maximum luminance; (d) Maximum efficiency.

5. ^{1}H- and ^{19}F-NMR spectra and high resolution mass spectrometers (HRMS) of all new compounds

Z1:

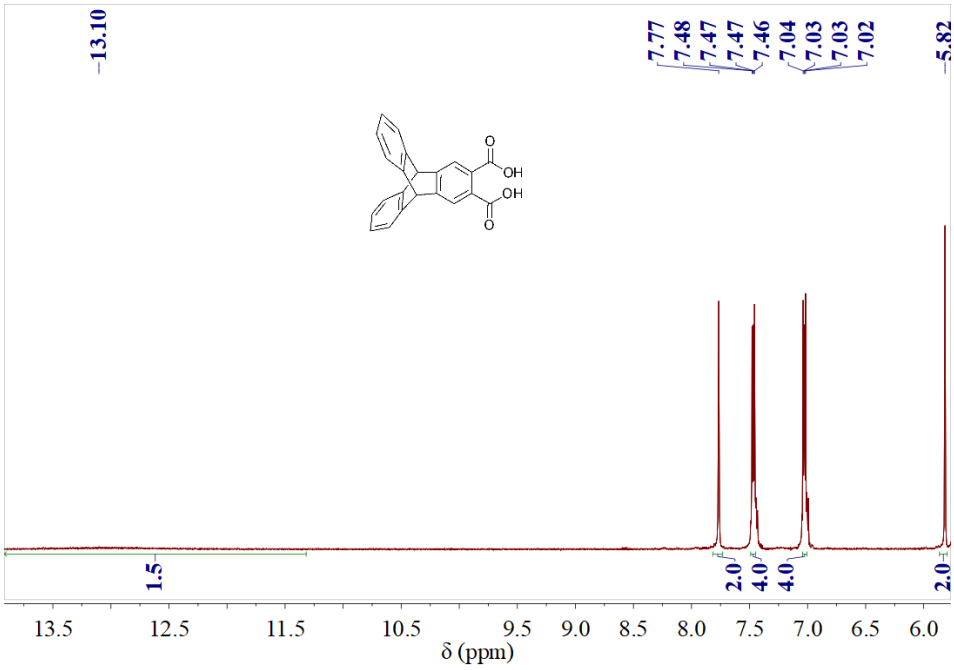

Z2:

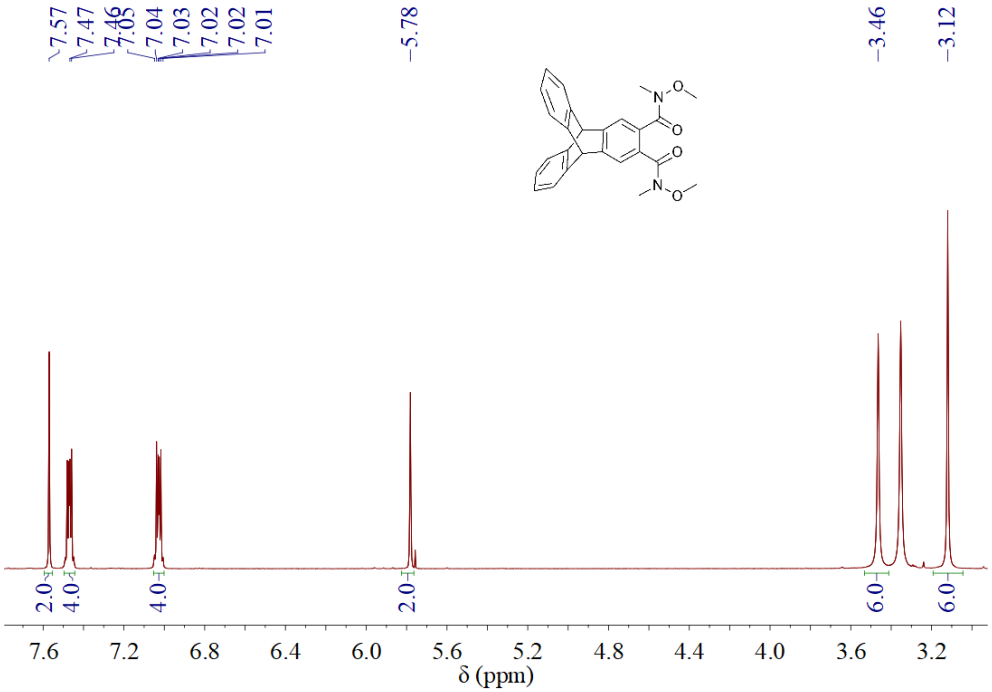
7.57
7.47
7.46
7.05
7.04
7.03
7.02
7.02
7.01
5.78
3.46
3.12
2.0
4.0
4.0
2.0
6.0
6.0
7.6
7.2
6.8
6.4
6.0
5.6
5.2
4.8
4.4
4.0
3.6
3.2
δ (ppm)

Z3:

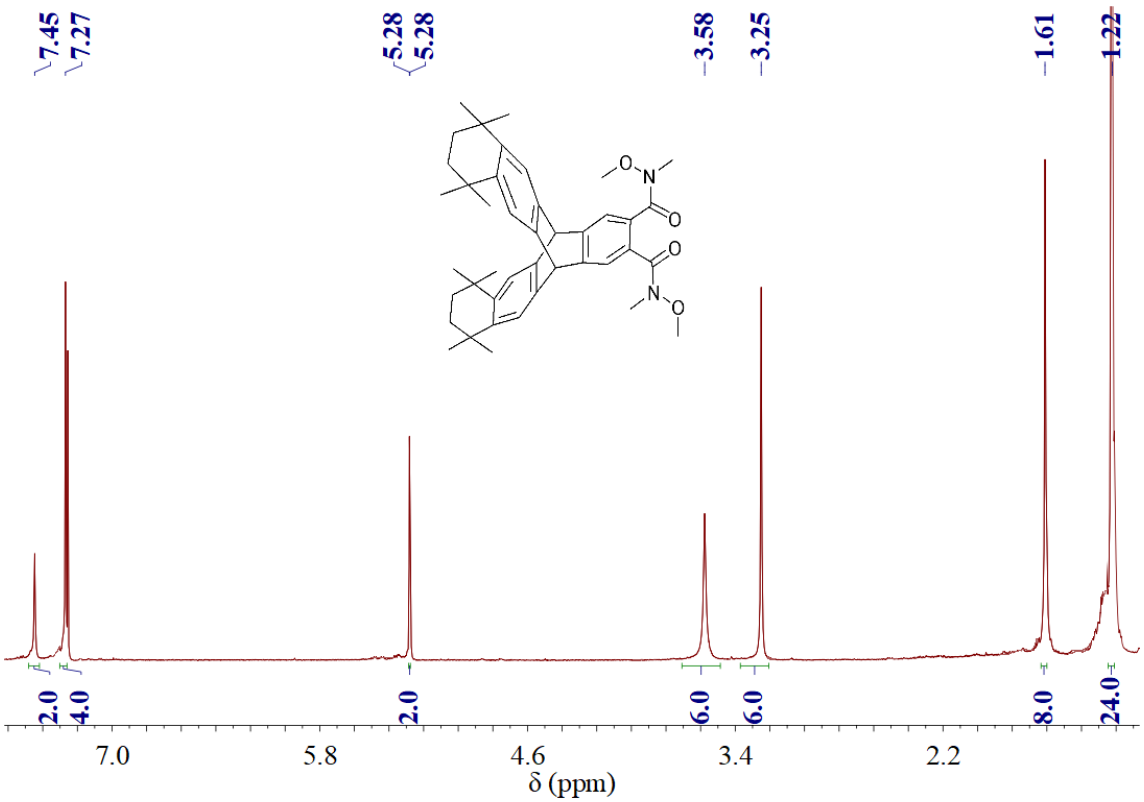
7.45
7.27
5.28
5.28
3.58
3.25
1.61
1.22
2.0
4.0
2.0
6.0
6.0
8.0
24.0
7.0
5.8
4.6
3.4
2.2
δ (ppm)

Z4:

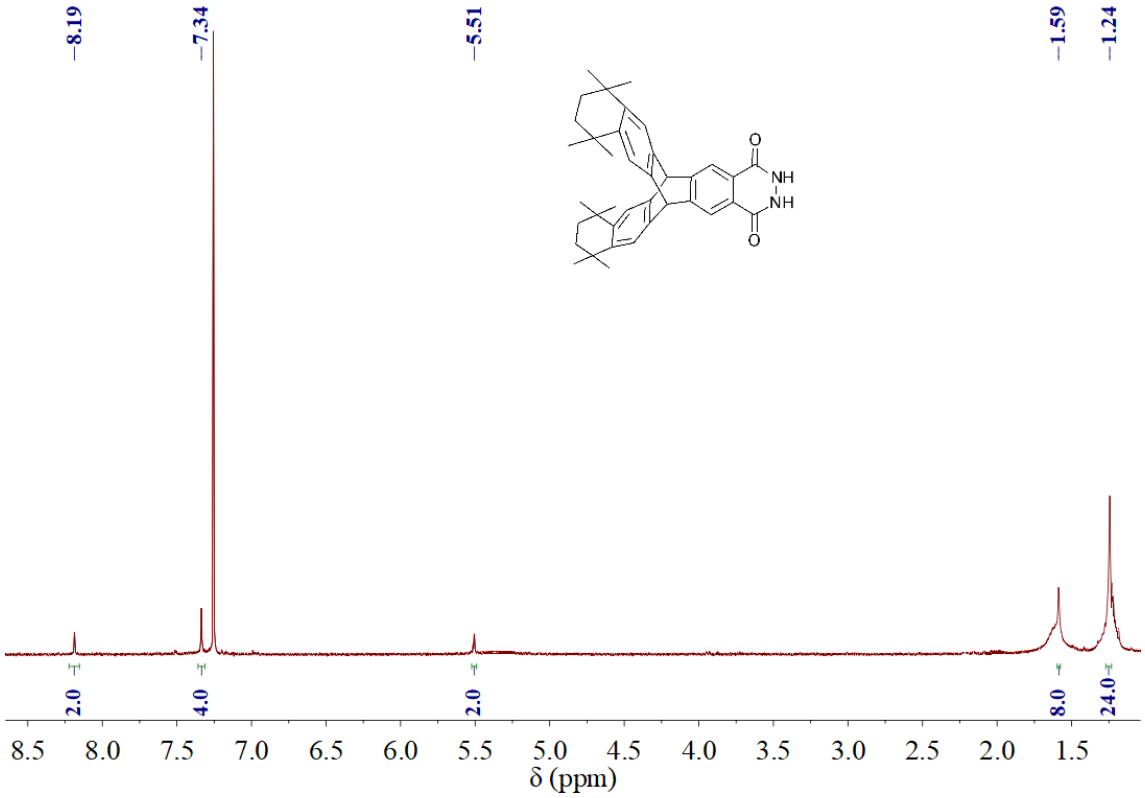
8.19
7.34
5.51
1.59
1.24
NH
NH
O
O
2.0
4.0
2.0
8.0
24.0
8.5 8.0 7.5 7.0 6.5 6.0 5.5 5.0 4.5 4.0 3.5 3.0 2.5 2.0 1.5
δ (ppm)

L1:

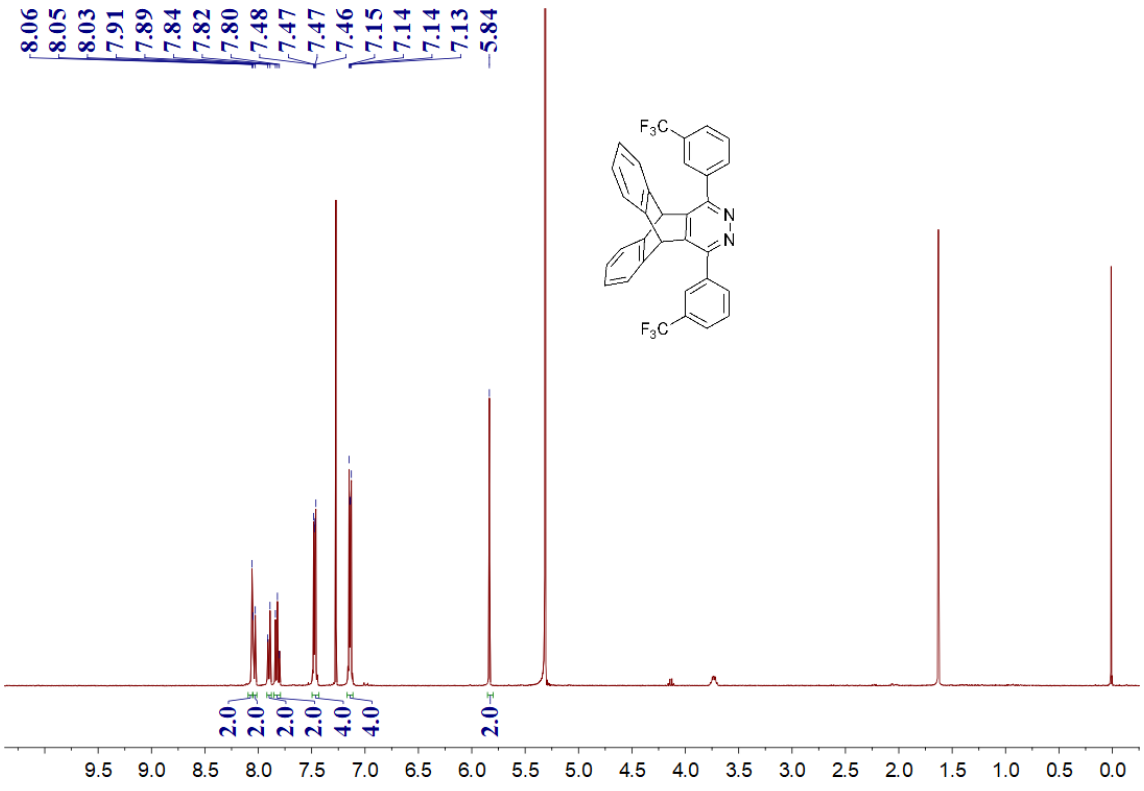
8.06
8.05
8.03
7.91
7.89
7.84
7.82
7.80
7.48
7.47
7.47
7.46
7.15
7.14
7.14
7.13
5.84
F3C
N
N
F3C
2.0
2.0
2.0
2.0
4.0
4.0
2.0
9.5 9.0 8.5 8.0 7.5 7.0 6.5 6.0 5.5 5.0 4.5 4.0 3.5 3.0 2.5 2.0 1.5 1.0 0.5 0.0

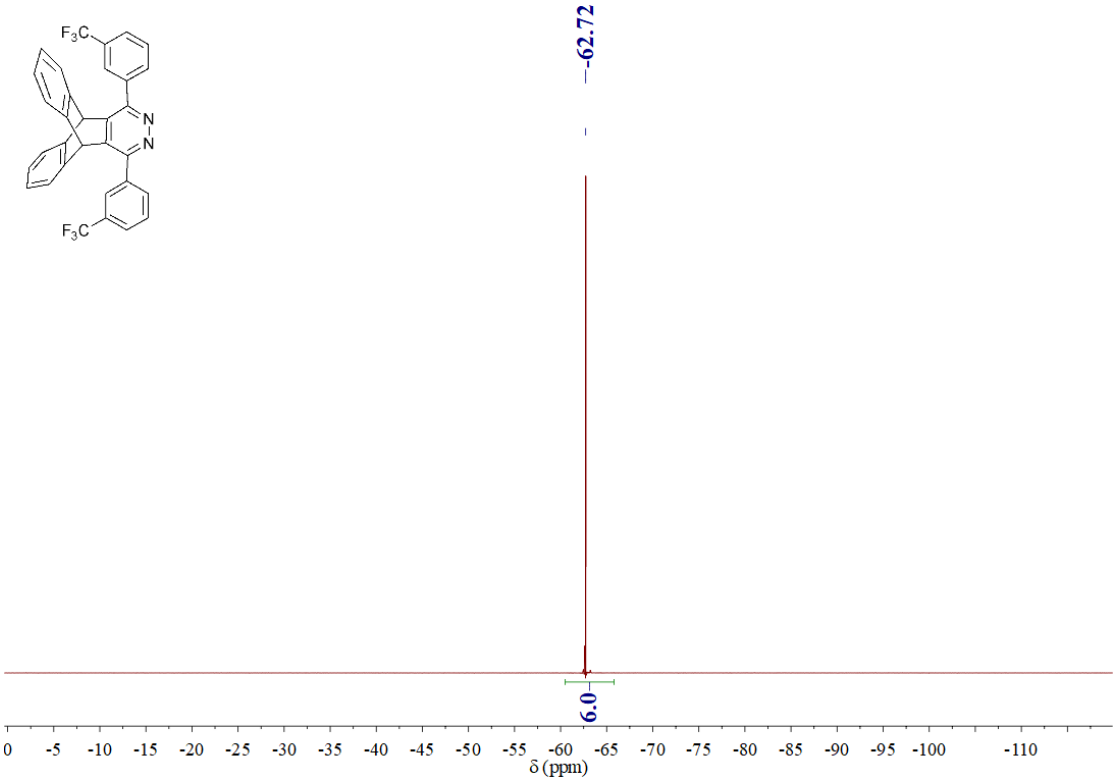
F3C
N
N
F3C
-62.72
6.0
0 -5 -10 -15 -20 -25 -30 -35 -40 -45 -50 -55 -60 -65 -70 -75 -80 -85 -90 -95 -100 -110
δ (ppm)

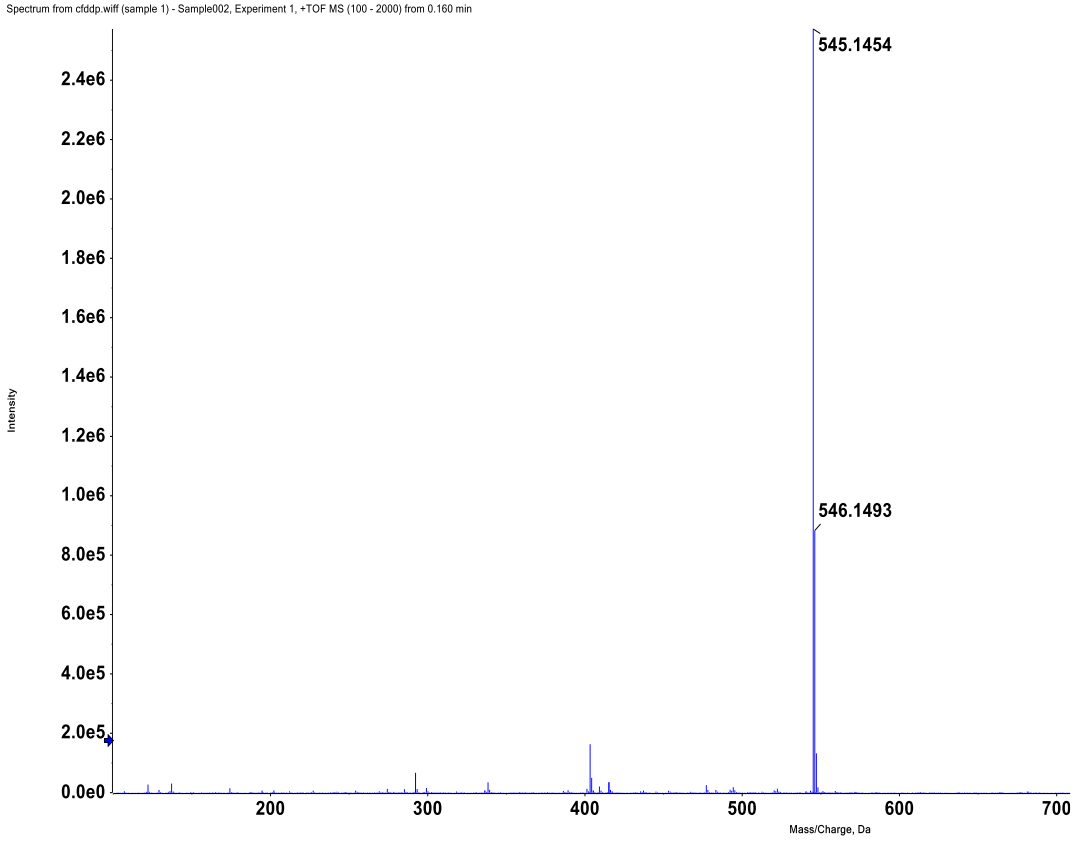
Spectrum from cfddp.wiff (sample 1) - Sample002, Experiment 1, +TOF MS (100 - 2000) from 0.160 min
545.1454
546.1493
Intensity
2.4e6
2.2e6
2.0e6
1.8e6
1.6e6
1.4e6
1.2e6
1.0e6
8.0e5
6.0e5
4.0e5
2.0e5
0.0e0
200 300 400 500 600 700
Mass/Charge, Da

L2:

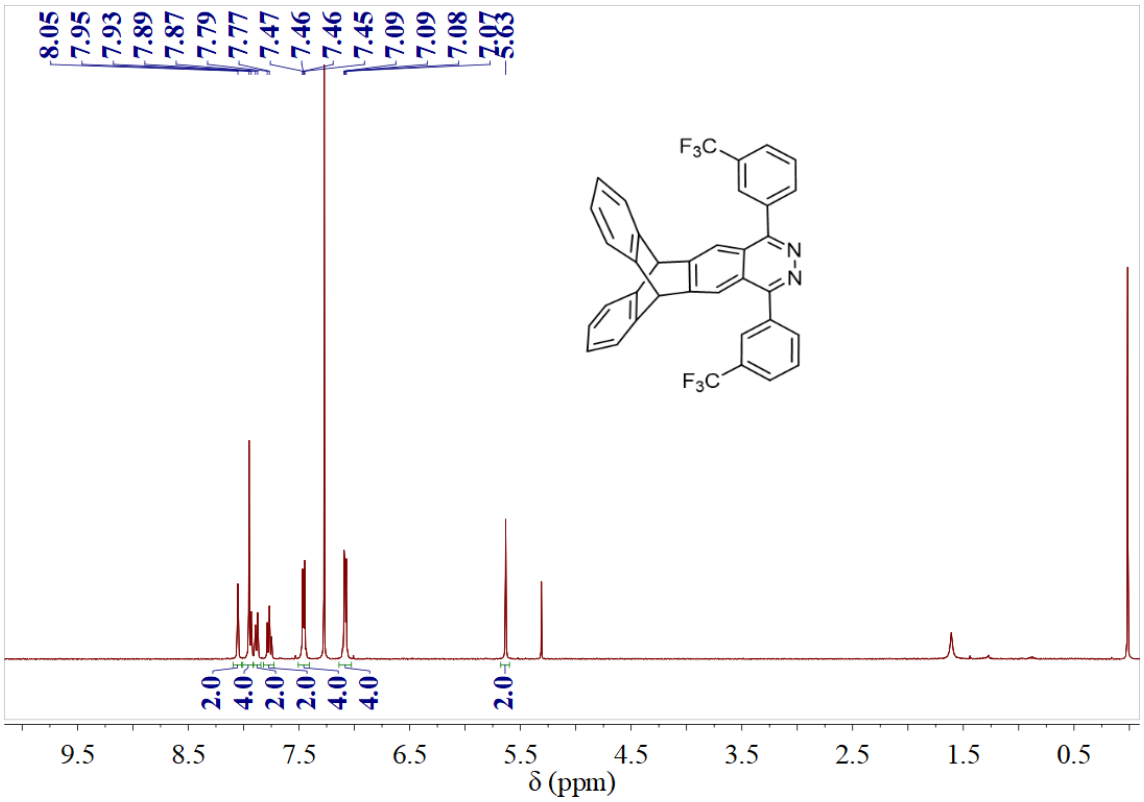
8.05
7.95
7.93
7.89
7.87
7.79
7.77
7.47
7.46
7.46
7.45
7.09
7.09
7.08
7.07
5.63
F3C
N
N
F3C
2.0
4.0
2.0
2.0
4.0
4.0
2.0
9.5
8.5
7.5
6.5
5.5
4.5
3.5
2.5
1.5
0.5
δ (ppm)

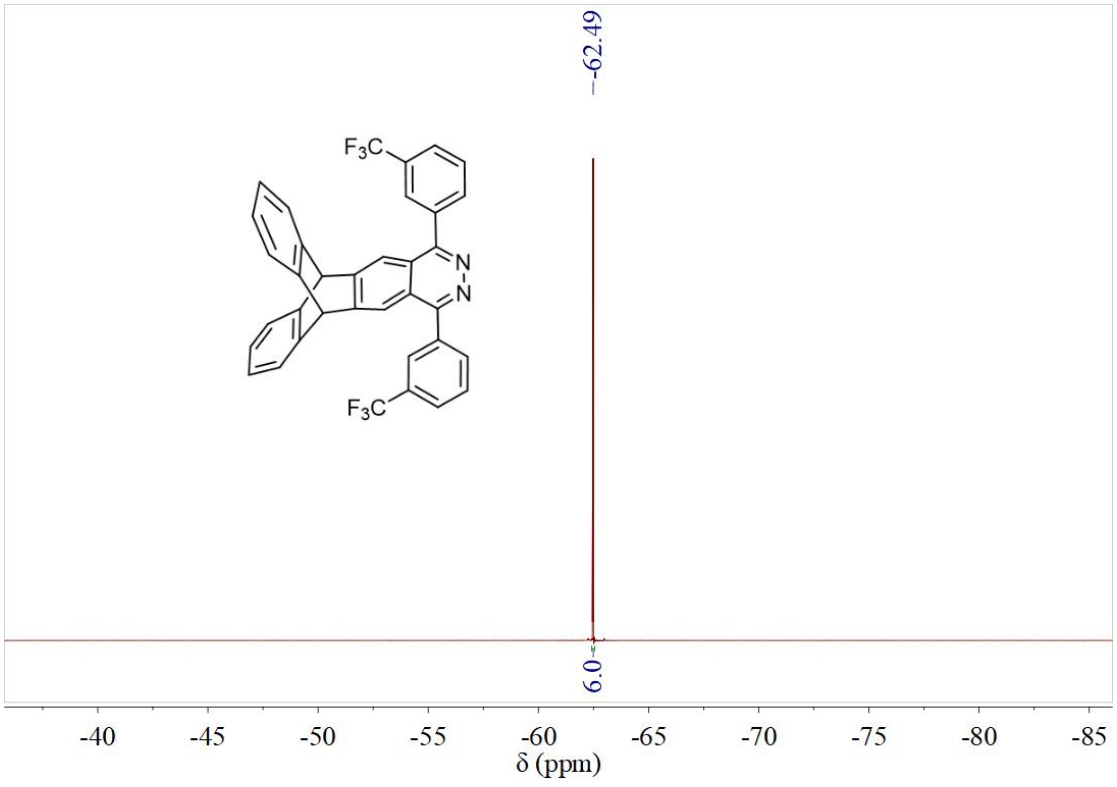
-62.49
F3C
N
N
F3C
6.0
-40
-45
-50
-55
-60
-65
-70
-75
-80
-85
δ (ppm)

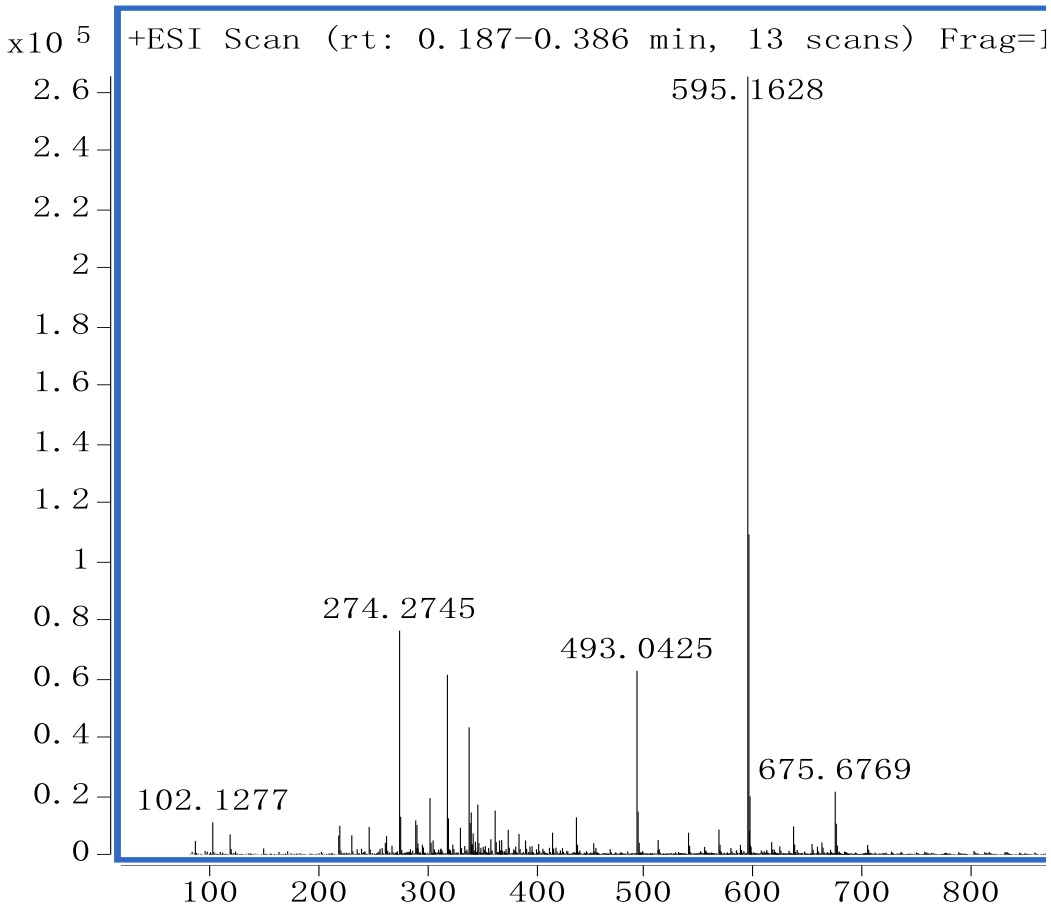
x10 5
+ESI Scan (rt: 0.187-0.386 min, 13 scans) Frag=1
595.1628
274.2745
493.0425
675.6769
102.1277

L3:

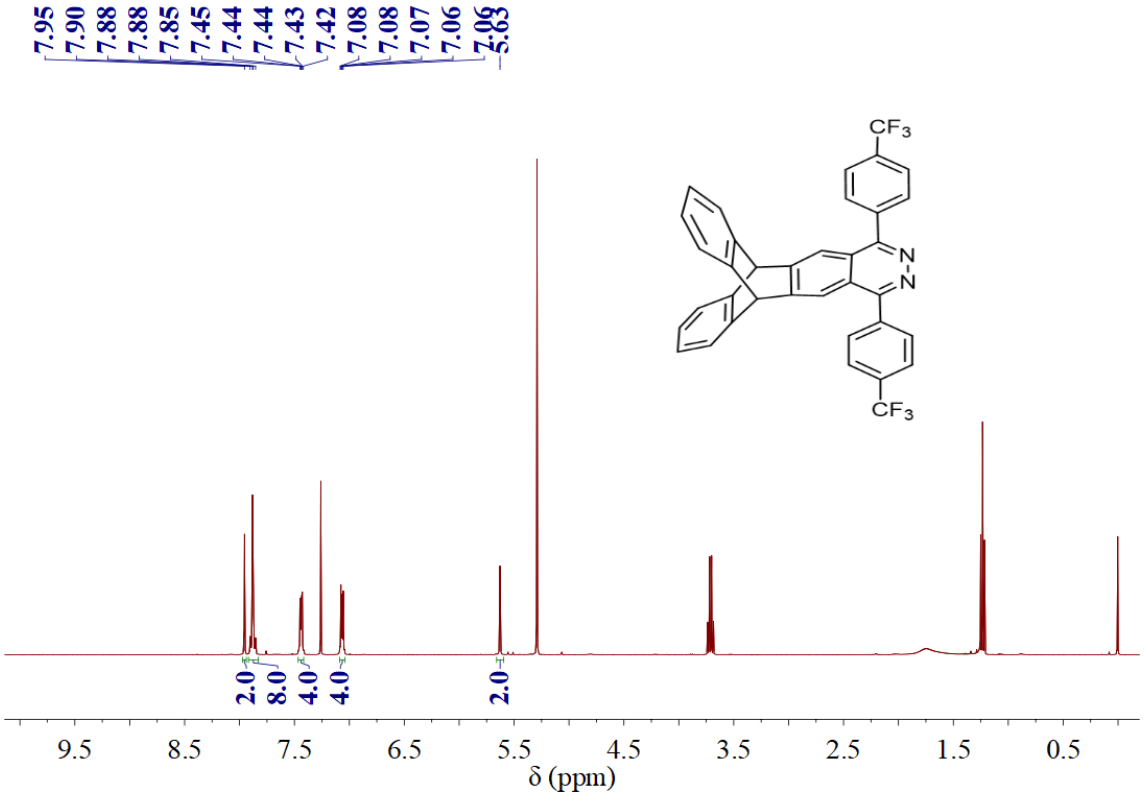
7.95
7.90
7.88
7.88
7.85
7.45
7.44
7.44
7.43
7.42
7.08
7.08
7.07
7.06
7.06
5.63
CF3
N
N
CF3
2.0
8.0
4.0
4.0
2.0
δ (ppm)

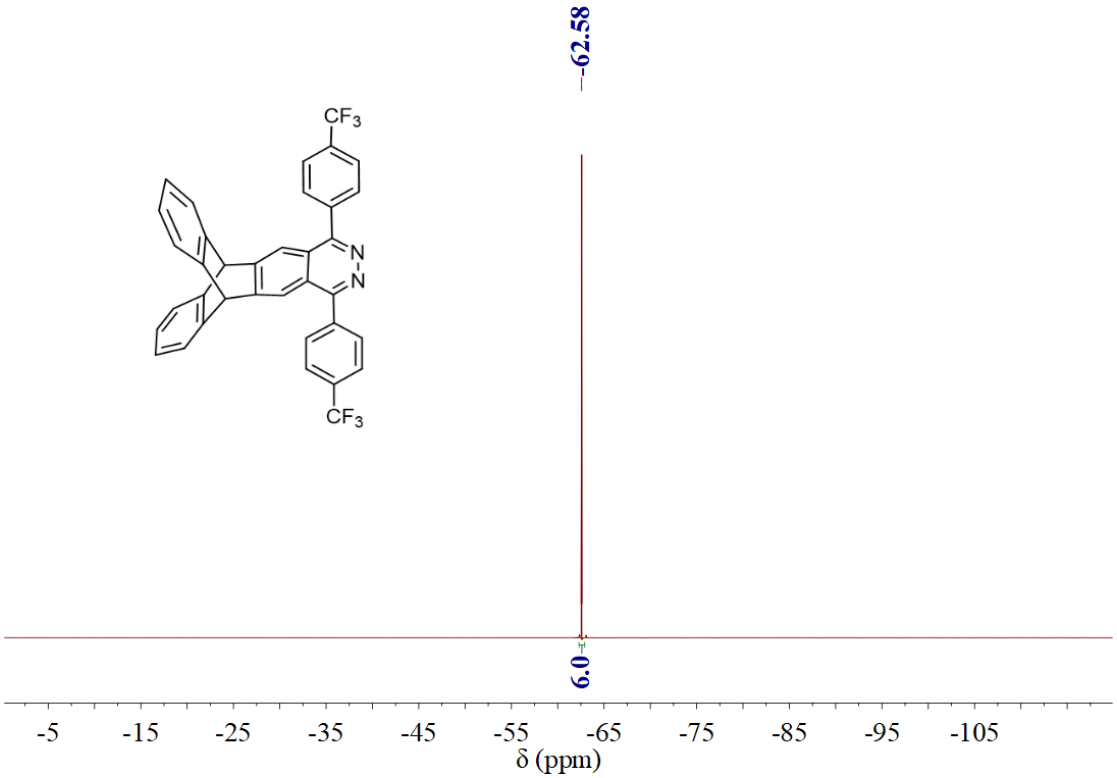
CF3
N
N
CF3
-62.58
6.0
-5
-15
-25
-35
-45
-55
-65
-75
-85
-95
-105
δ (ppm)

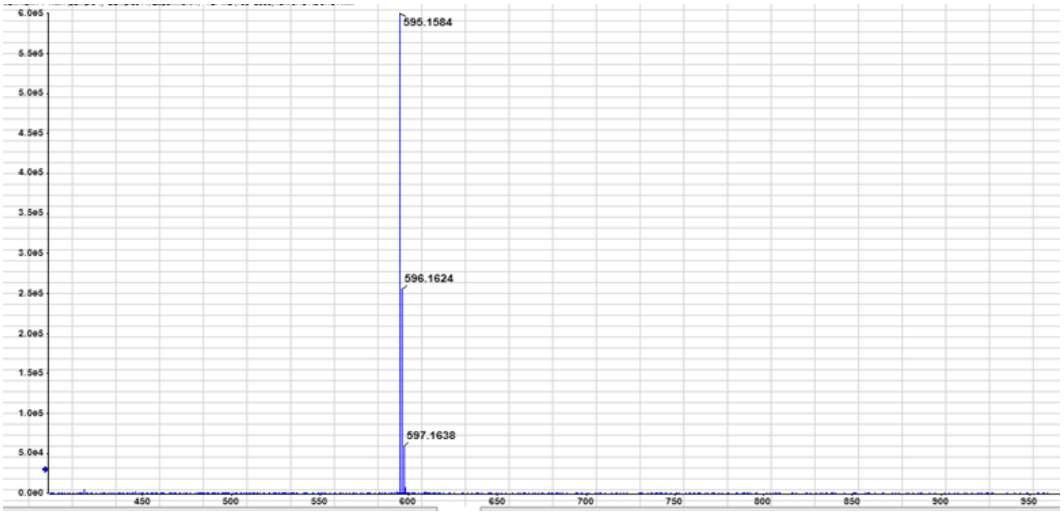
595.1584
596.1624
597.1638

L4:

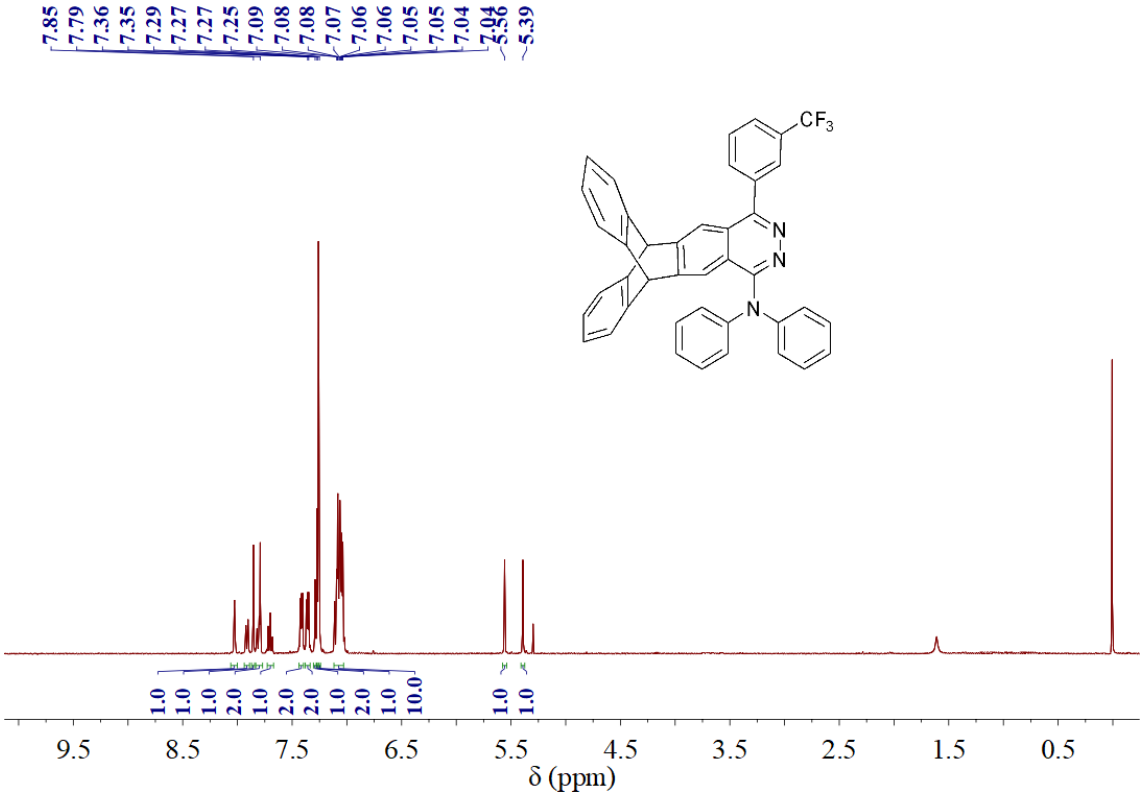
7.85
7.79
7.36
7.35
7.29
7.27
7.27
7.25
7.09
7.08
7.08
7.07
7.06
7.06
7.05
7.05
7.04
7.04
5.56
5.39
CF3
N
N
N
1.0
1.0
1.0
2.0
1.0
2.0
2.0
1.0
2.0
1.0
10.0
1.0
1.0
9.5
8.5
7.5
6.5
5.5
4.5
3.5
2.5
1.5
0.5
δ (ppm)

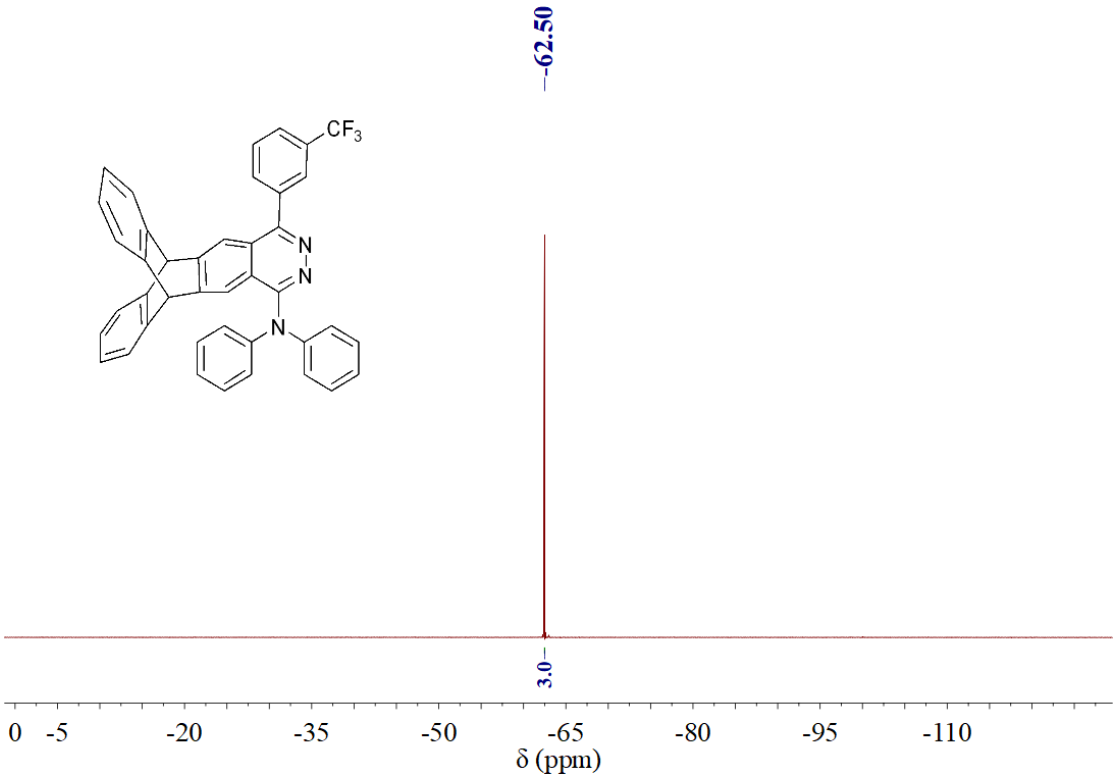
-62.50
CF3
N
N
N
3.0
0
-5
-20
-35
-50
-65
-80
-95
-110
δ (ppm)

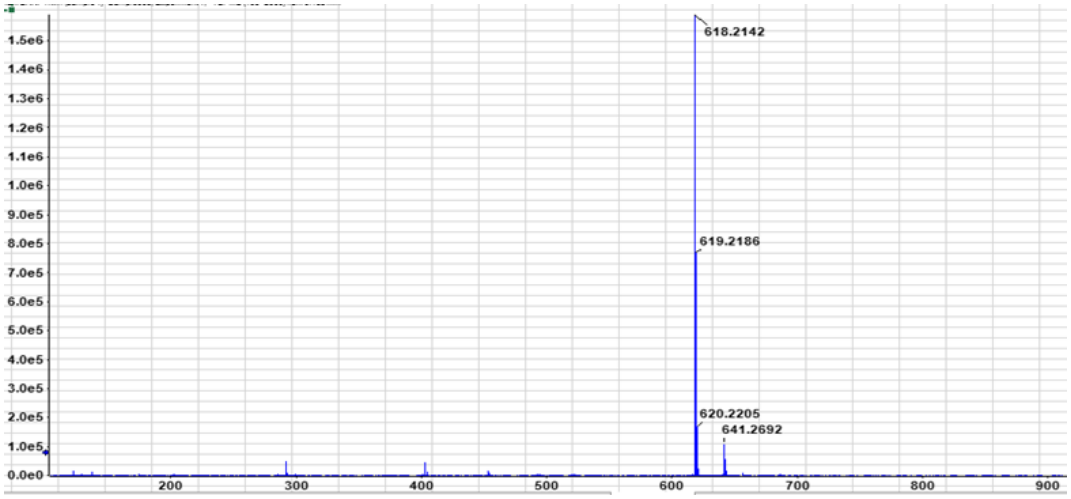
618.2142
619.2186
620.2205
641.2692

L5:

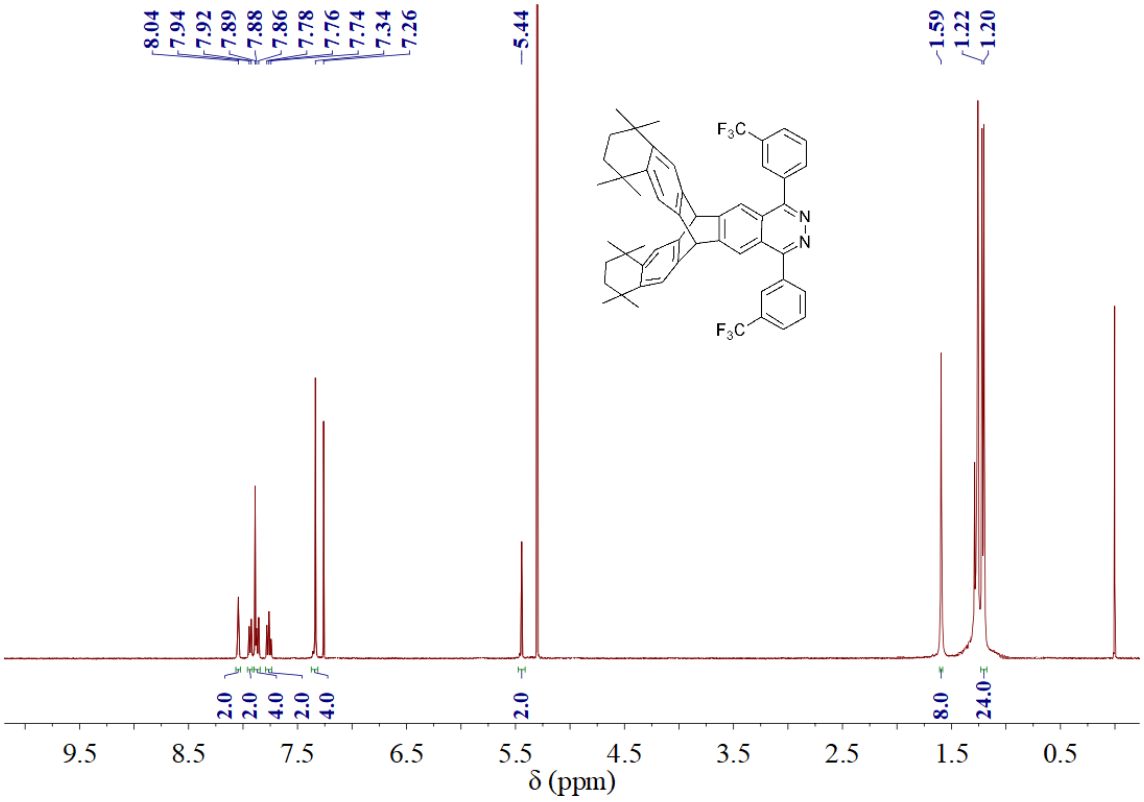
8.04
7.94
7.92
7.89
7.88
7.86
7.78
7.76
7.74
7.34
7.26
5.44
1.59
1.22
1.20
F3C
N
N
F3C
2.0
2.0
4.0
2.0
4.0
2.0
8.0
24.0
9.5
8.5
7.5
6.5
5.5
4.5
3.5
2.5
1.5
0.5
δ (ppm)

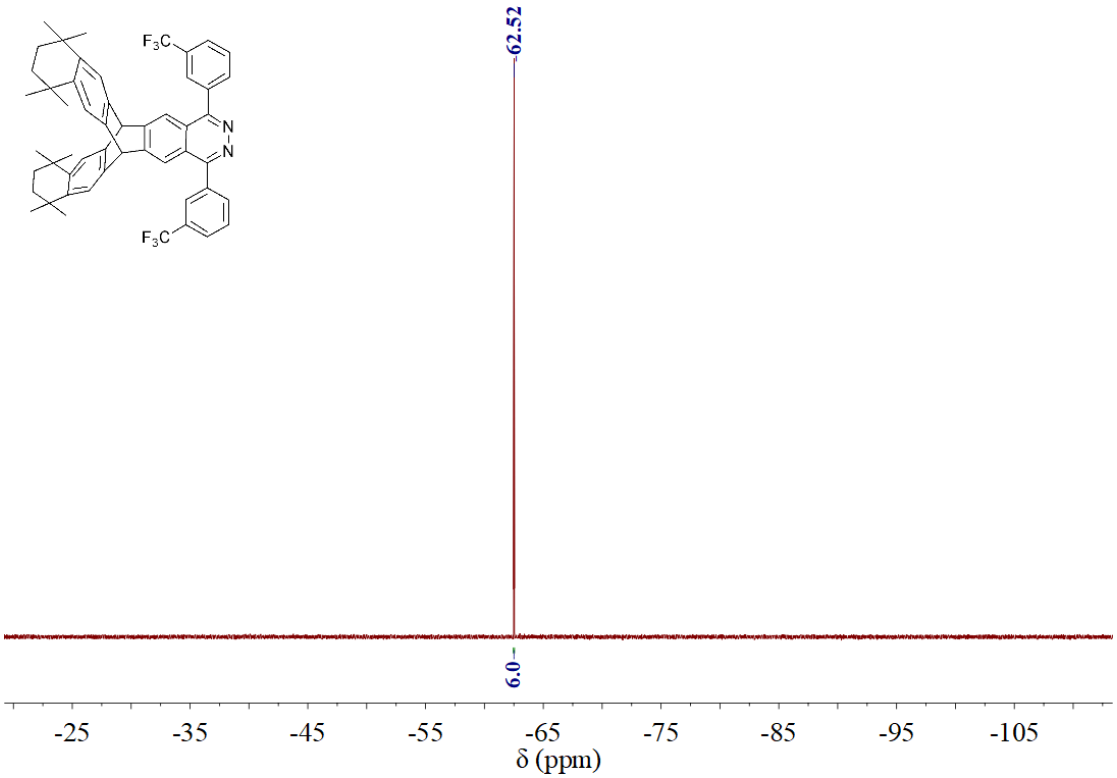
F3C
N
N
F3C
62.52
6.0
-25
-35
-45
-55
-65
-75
-85
-95
-105
δ (ppm)

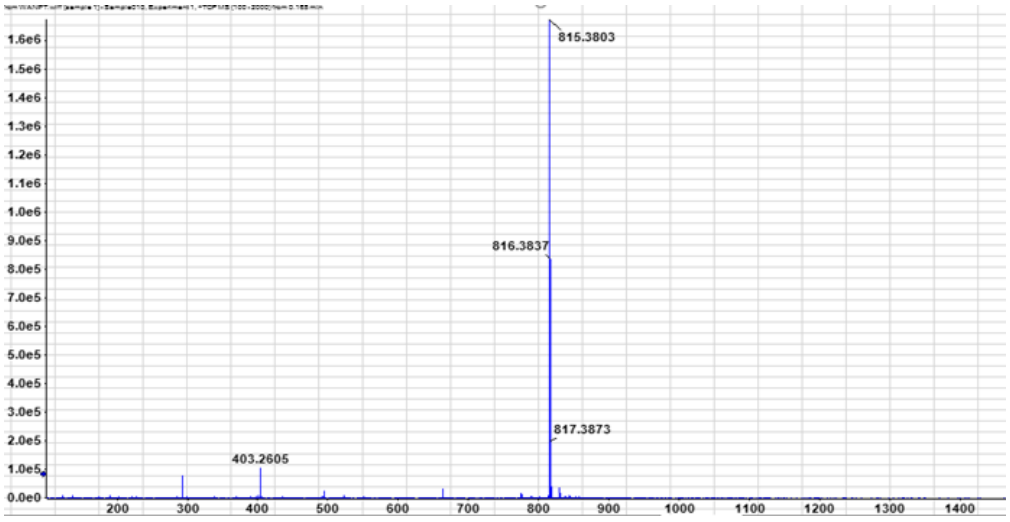
815.3803
816.3837
817.3873
403.2605
1.6e6
1.5e6
1.4e6
1.3e6
1.2e6
1.1e6
1.0e6
9.0e5
8.0e5
7.0e5
6.0e5
5.0e5
4.0e5
3.0e5
2.0e5
1.0e5
0.0e0
200
300
400
500
600
700
800
900
1000
1100
1200
1300
1400

Ir1:

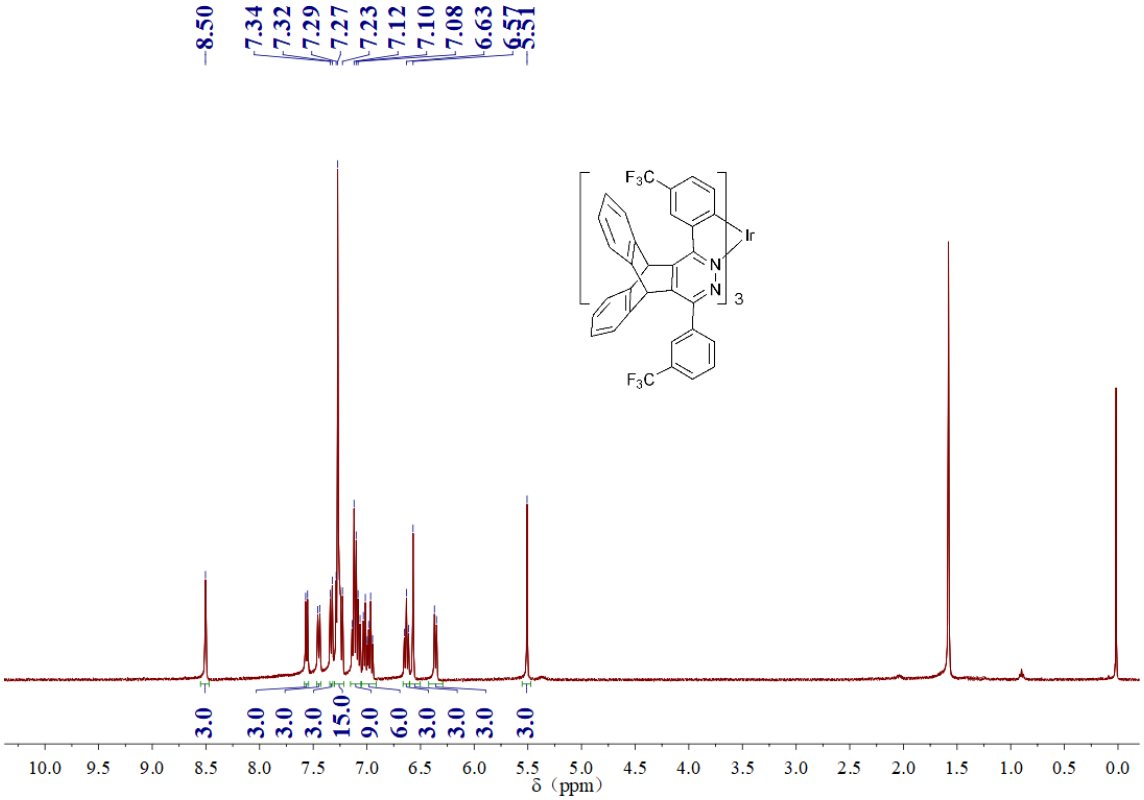
8.50
7.34
7.32
7.29
7.27
7.23
7.12
7.10
7.08
6.63
6.57
5.51
F3C
Ir
N
N
3
F3C
3.0
3.0
3.0
3.0
15.0
9.0
6.0
3.0
3.0
3.0
3.0
10.0 9.5 9.0 8.5 8.0 7.5 7.0 6.5 6.0 5.5 5.0 4.5 4.0 3.5 3.0 2.5 2.0 1.5 1.0 0.5 0.0
δ (ppm)

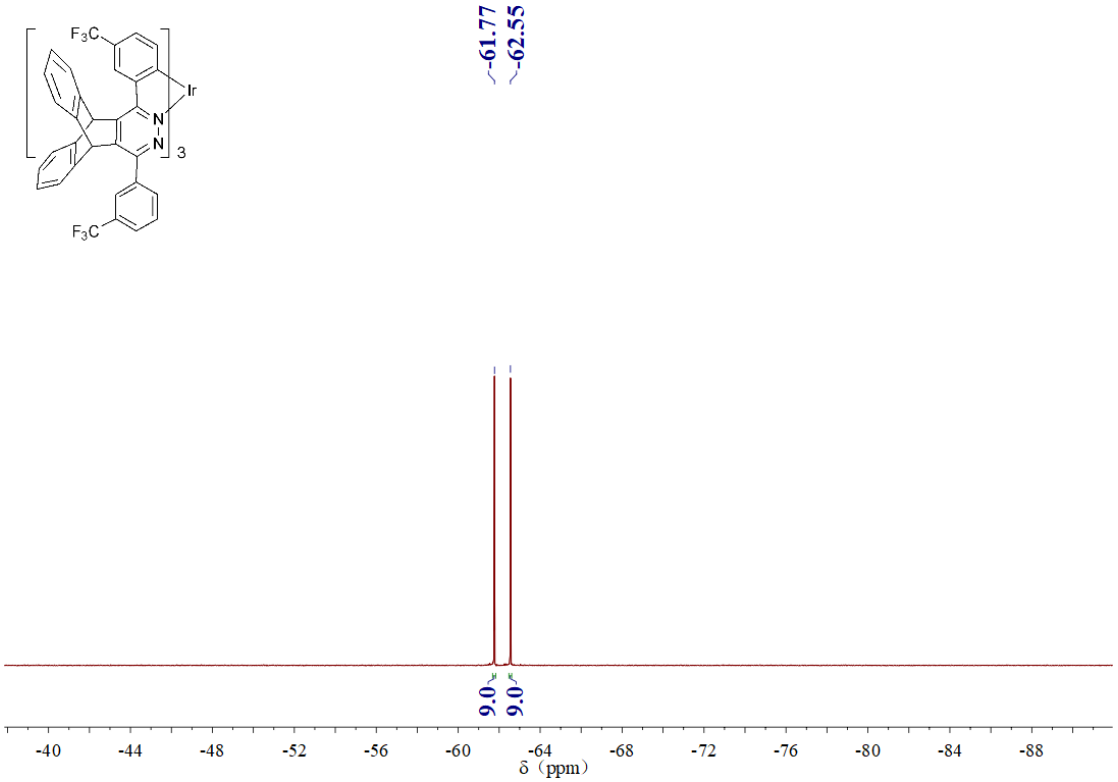
F3C
Ir
N
N
3
F3C
-61.77
-62.55
9.0
9.0
-40 -44 -48 -52 -56 -60 -64 -68 -72 -76 -80 -84 -88
δ (ppm)

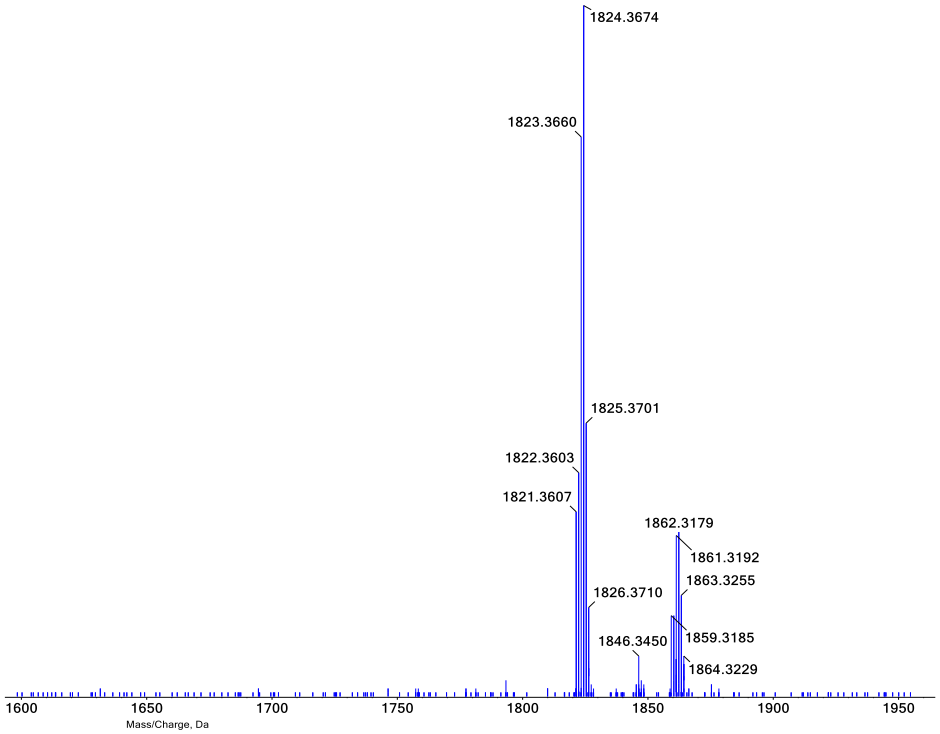
1824.3674
1823.3660
1825.3701
1822.3603
1821.3607
1862.3179
1861.3192
1863.3255
1826.3710
1846.3450
1859.3185
1864.3229
1600
1650
1700
1750
1800
1850
1900
1950
Mass/Charge, Da

Ir2:

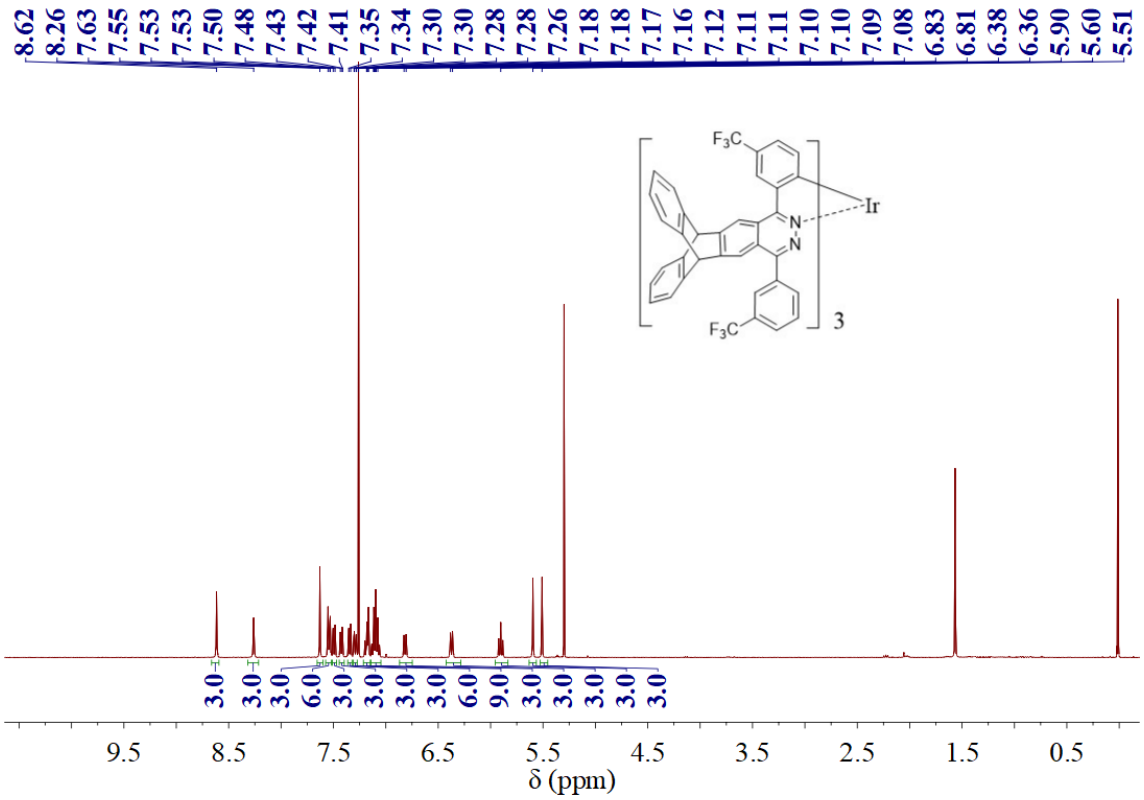
8.62
8.26
7.63
7.55
7.53
7.53
7.50
7.48
7.43
7.42
7.41
7.35
7.34
7.30
7.30
7.28
7.28
7.26
7.18
7.18
7.17
7.16
7.12
7.11
7.11
7.10
7.10
7.09
7.08
6.83
6.81
6.38
6.36
5.90
5.60
5.51
F3C
Ir
N
N
F3C
3
3.0
3.0
3.0
6.0
3.0
3.0
3.0
3.0
6.0
9.0
3.0
3.0
3.0
3.0
3.0
9.5
8.5
7.5
6.5
5.5
4.5
3.5
2.5
1.5
0.5
δ (ppm)

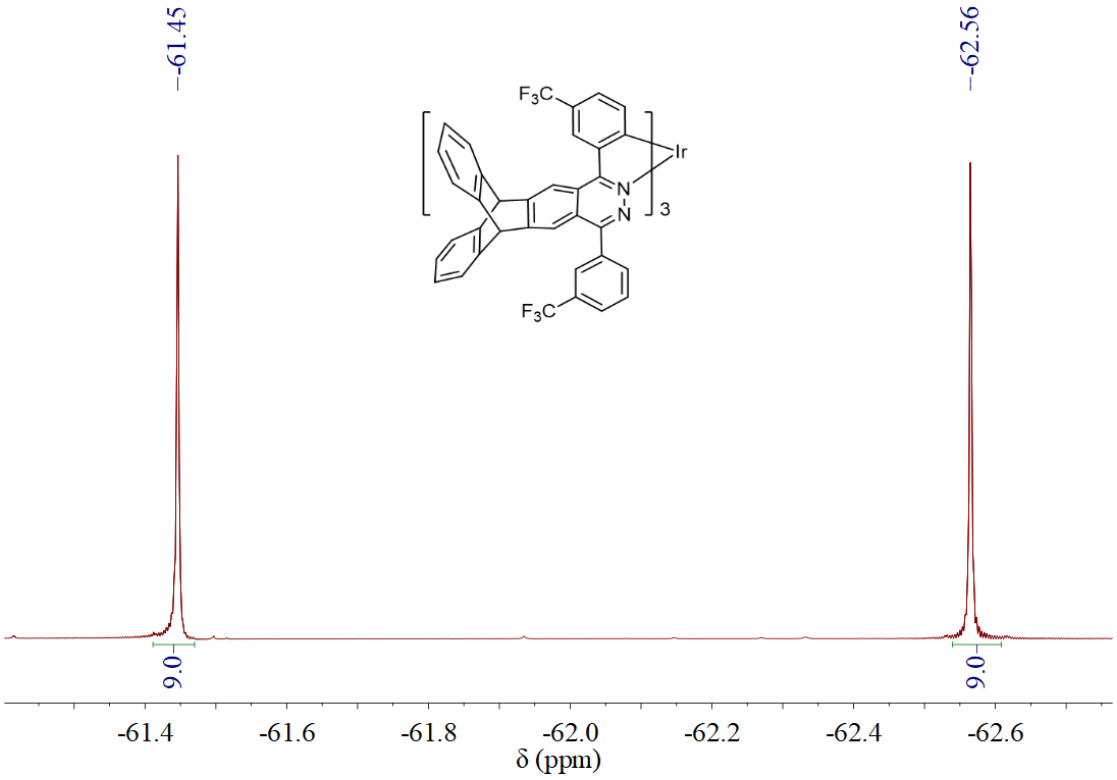
-61.45
-62.56
F3C
Ir
N
N
3
F3C
9.0
9.0
-61.4
-61.6
-61.8
-62.0
-62.2
-62.4
-62.6
δ (ppm)

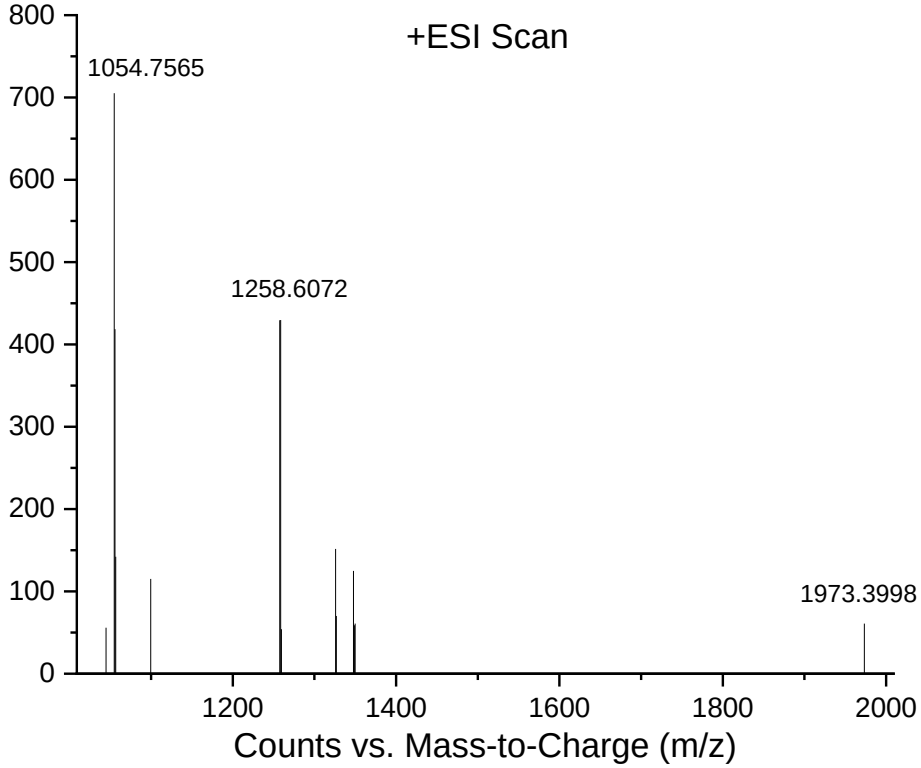
+ESI Scan
1054.7565
1258.6072
1973.3998
800
700
600
500
400
300
200
100
0
1200
1400
1600
1800
2000
Counts vs. Mass-to-Charge (m/z)

Ir3:

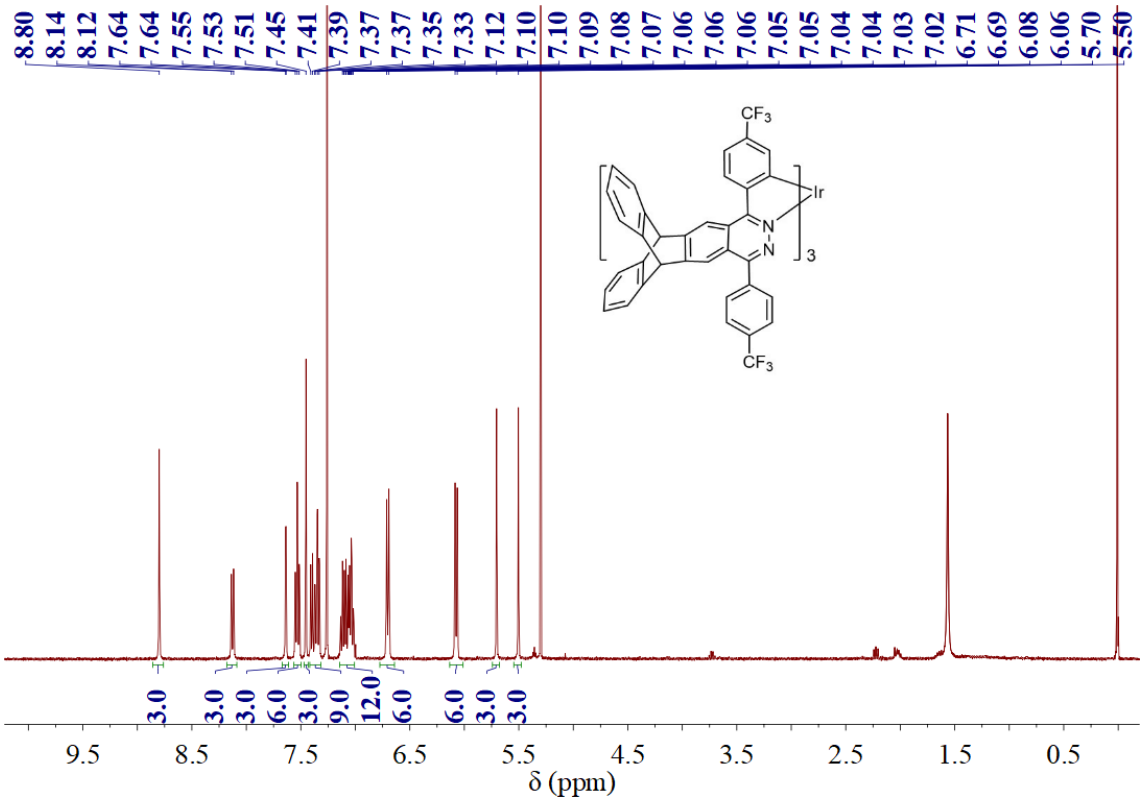
8.80
8.14
8.12
7.64
7.64
7.55
7.53
7.51
7.45
7.41
7.39
7.37
7.37
7.35
7.33
7.12
7.10
7.10
7.09
7.08
7.07
7.06
7.06
7.06
7.05
7.05
7.04
7.04
7.03
7.02
6.71
6.69
6.08
6.06
5.70
5.50
CF3
Ir
N
N
3
CF3
3.0
3.0
3.0
6.0
3.0
9.0
12.0
6.0
6.0
3.0
3.0
9.5
8.5
7.5
6.5
5.5
4.5
3.5
2.5
1.5
0.5
δ (ppm)

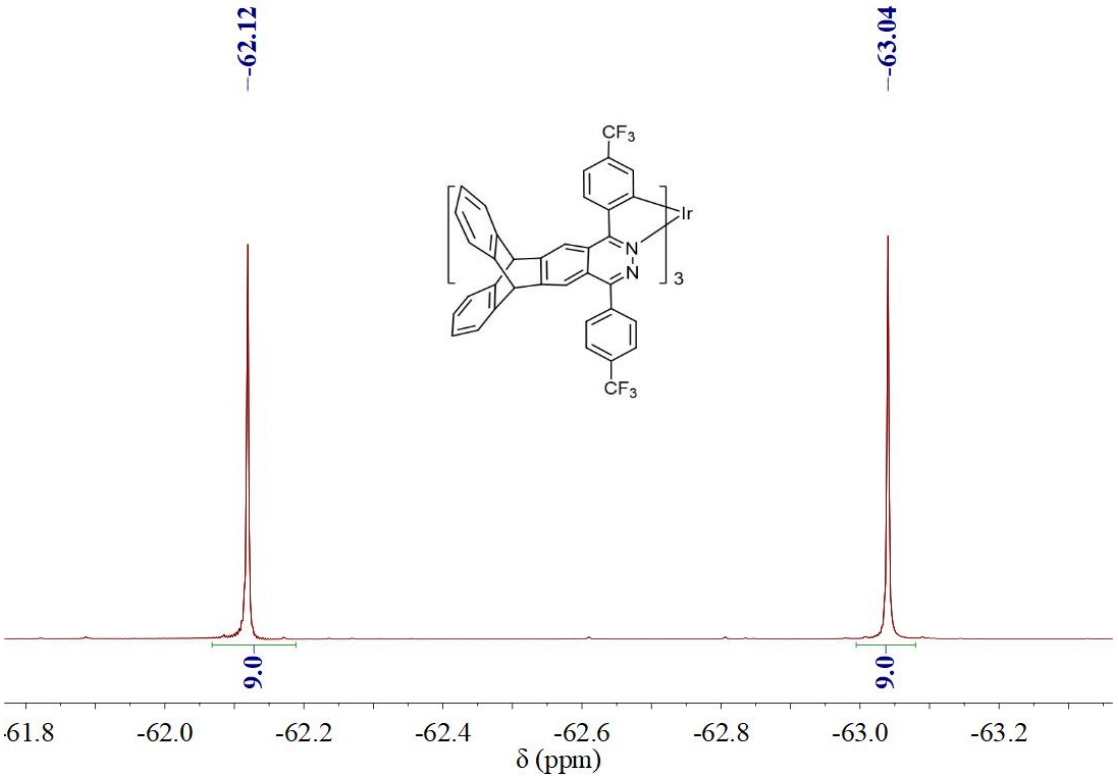
-62.12
-63.04
CF3
Ir
N
N
3
CF3
9.0
9.0
-61.8
-62.0
-62.2
-62.4
-62.6
-62.8
-63.0
-63.2
δ (ppm)

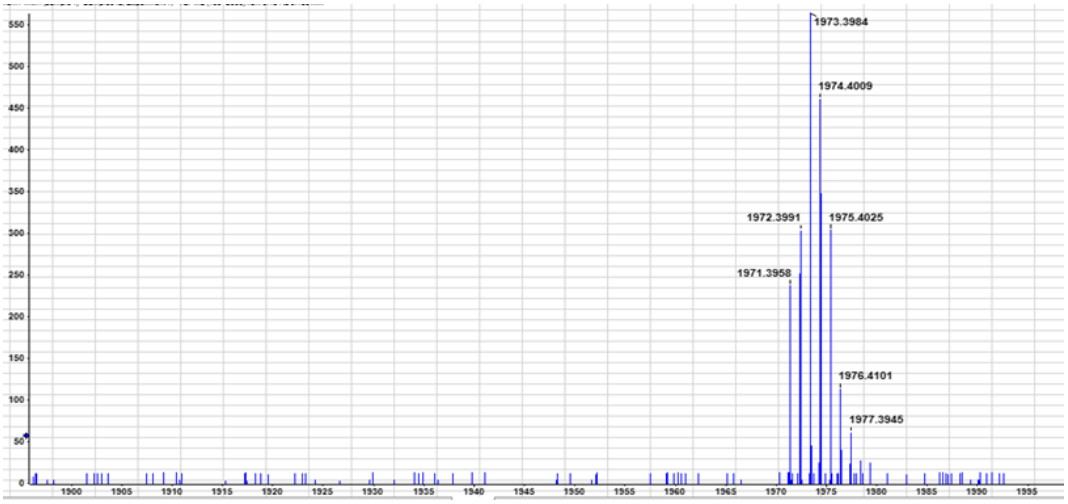
1973.3984
1974.4009
1972.3991
1975.4025
1971.3958
1976.4101
1977.3945

Ir4:

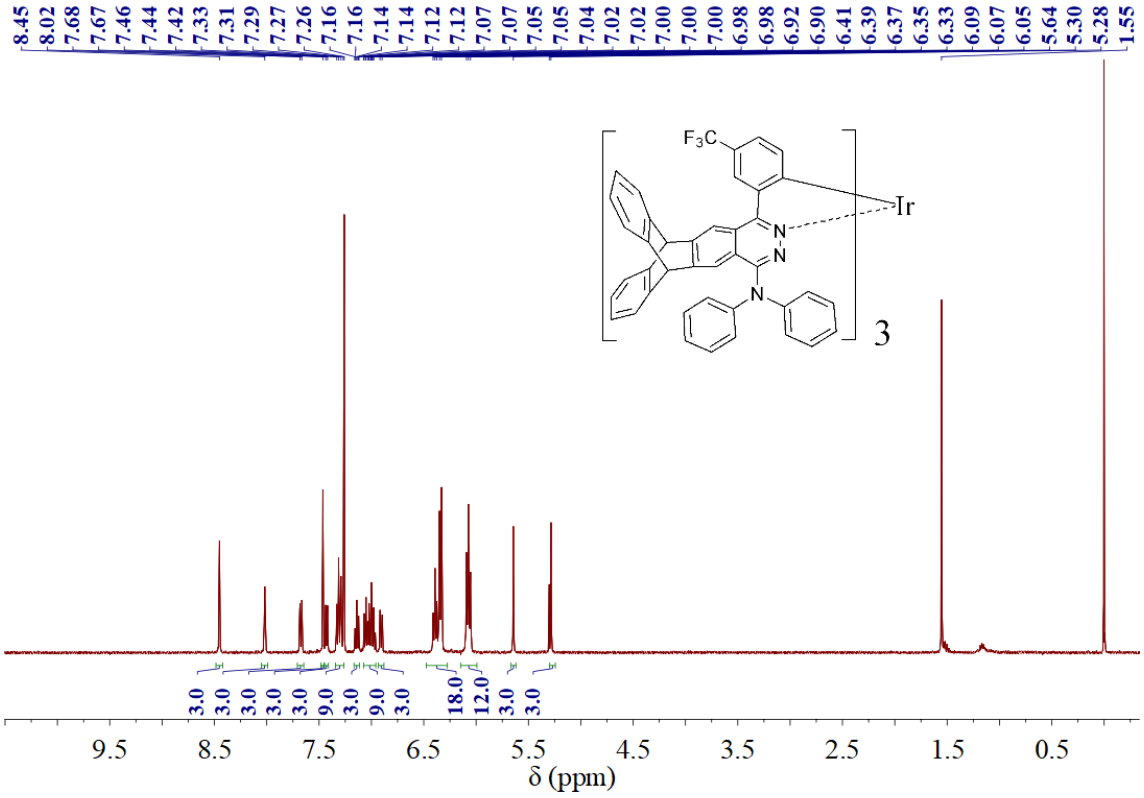
8.45
8.02
7.68
7.67
7.46
7.44
7.42
7.33
7.31
7.29
7.27
7.26
7.16
7.16
7.14
7.14
7.12
7.12
7.07
7.07
7.05
7.05
7.04
7.02
7.02
7.00
7.00
7.00
6.98
6.98
6.92
6.90
6.41
6.39
6.37
6.35
6.33
6.09
6.07
6.05
5.64
5.30
5.28
1.55
F3C
Ir
N
N
N
3
3.0
3.0
3.0
3.0
3.0
9.0
3.0
9.0
3.0
18.0
12.0
3.0
3.0
9.5
8.5
7.5
6.5
5.5
4.5
3.5
2.5
1.5
0.5
δ (ppm)

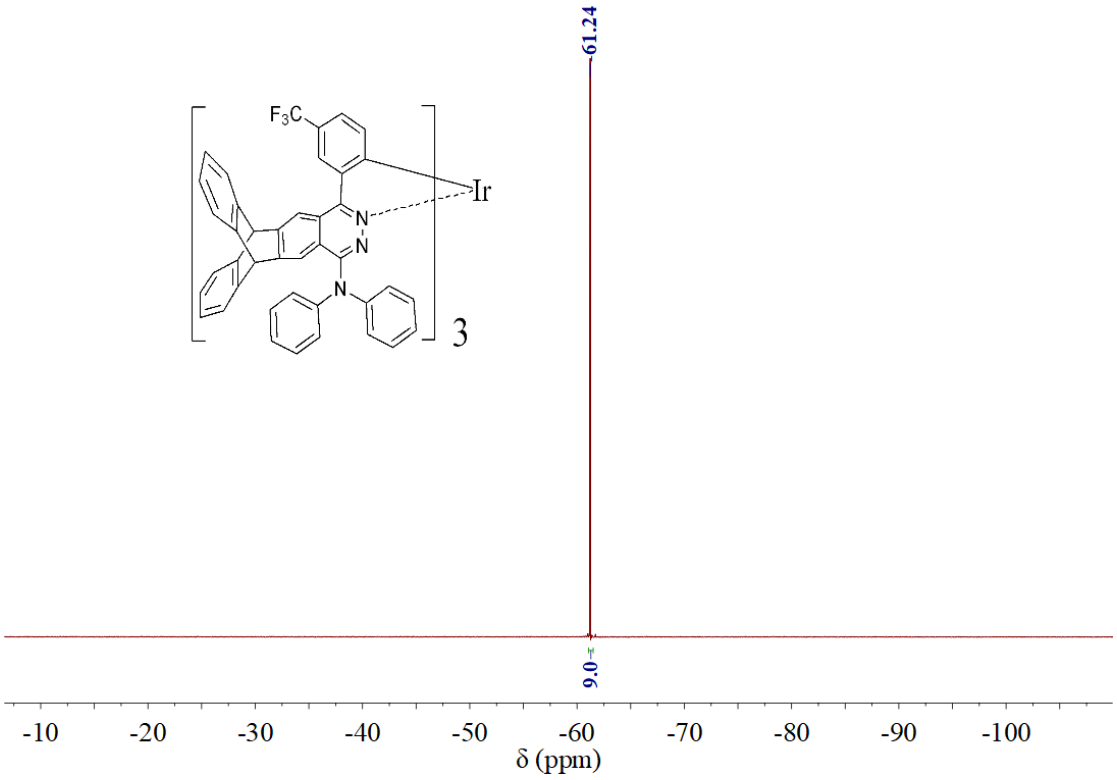
61.24
F3C
Ir
N
N
N
3
9.0
-10
-20
-30
-40
-50
-60
-70
-80
-90
-100
δ (ppm)

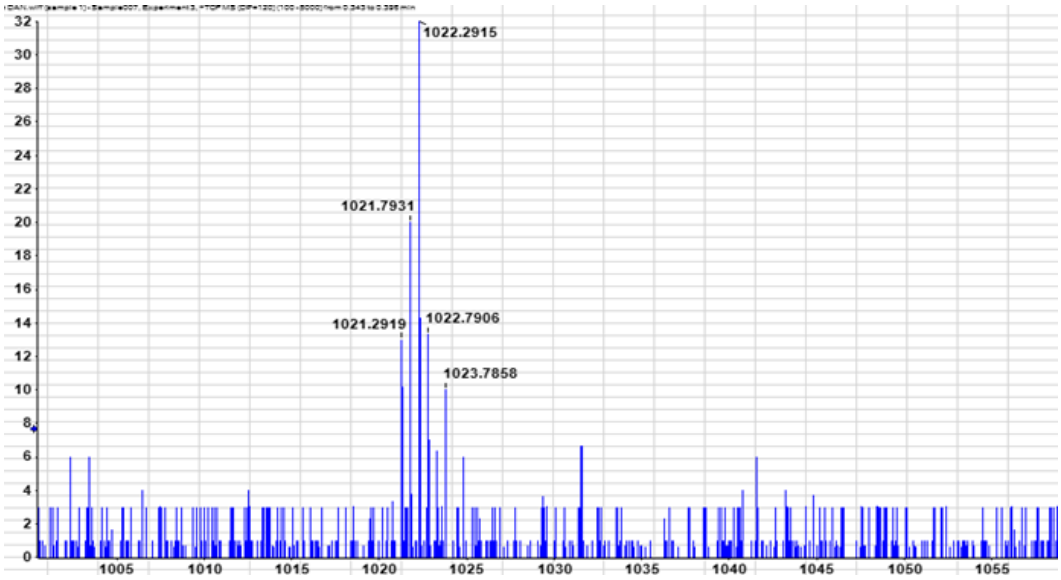
1022.2915
1021.7931
1021.2919
1022.7906
1023.7858
1005
1010
1015
1020
1025
1030
1035
1040
1045
1050
1055

Ir5:

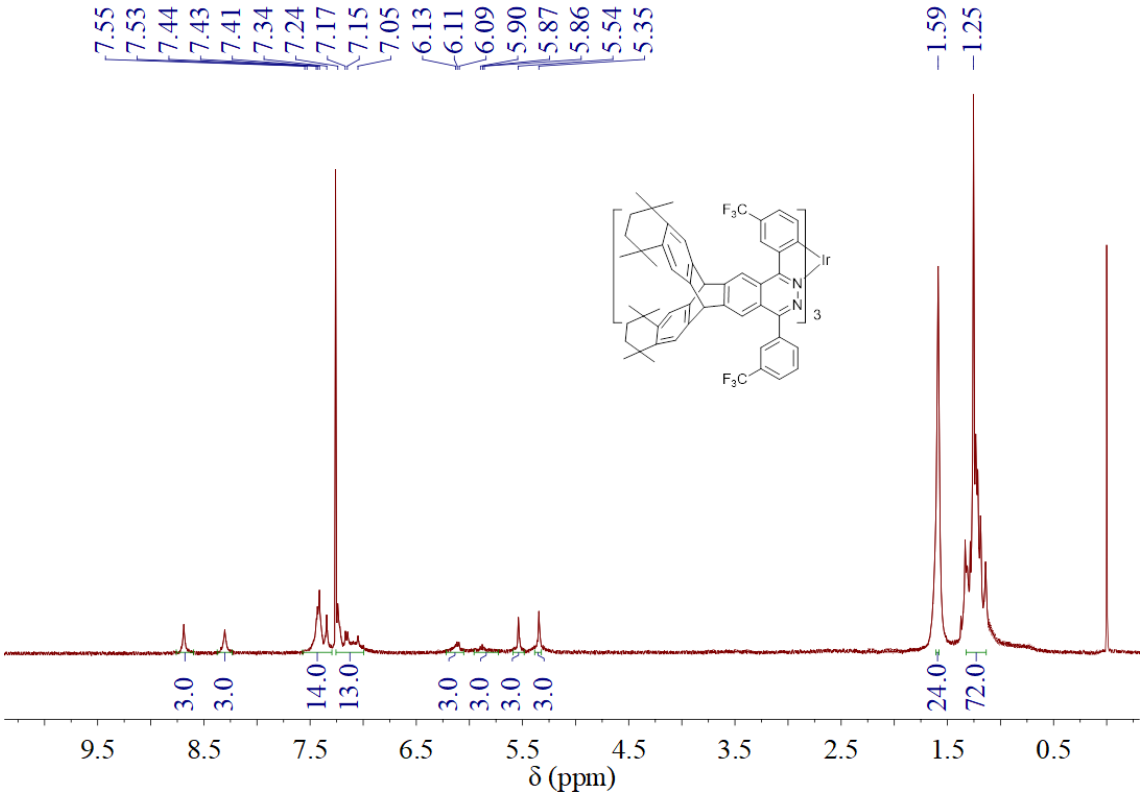
7.55
7.53
7.44
7.43
7.41
7.34
7.24
7.17
7.15
7.05
6.13
6.11
6.09
5.90
5.87
5.86
5.54
5.35
1.59
1.25
F3C
Ir
N
N
3
F3C
3.0
3.0
14.0
13.0
3.0
3.0
3.0
3.0
24.0
72.0
9.5
8.5
7.5
6.5
5.5
4.5
3.5
2.5
1.5
0.5
δ (ppm)

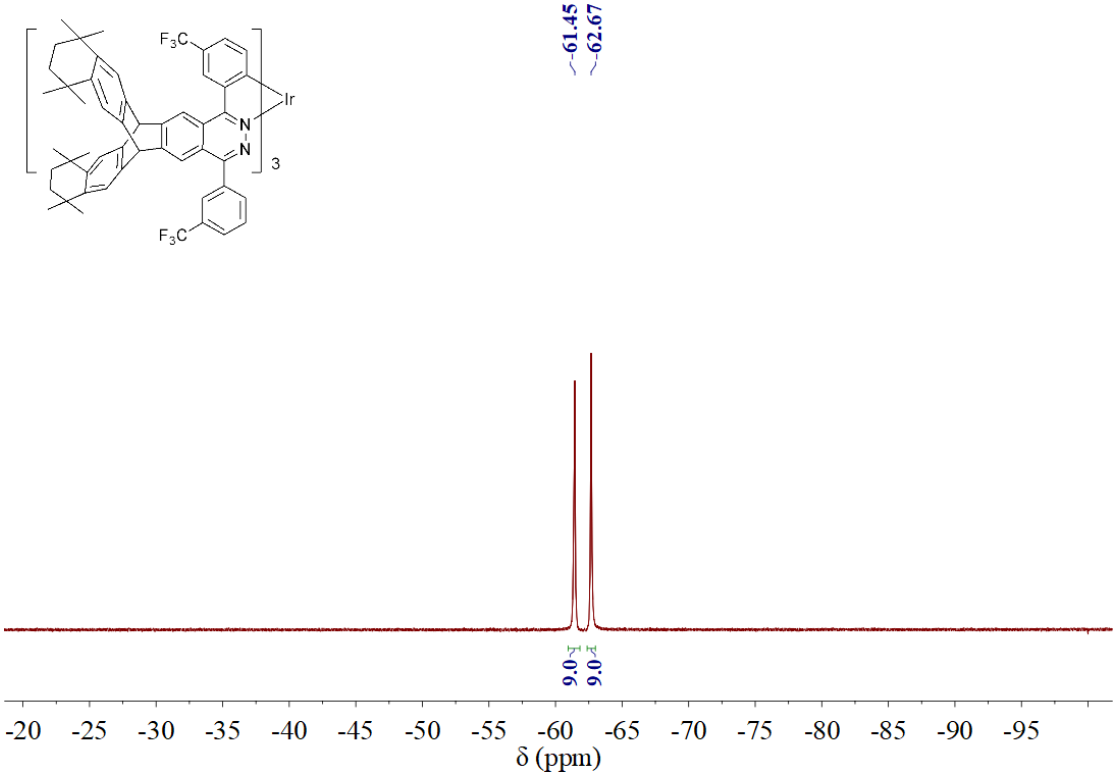
F3C
Ir
N
N
3
F3C
-61.45
-62.67
9.0
9.0
-20
-25
-30
-35
-40
-45
-50
-55
-60
-65
-70
-75
-80
-85
-90
-95
δ (ppm)

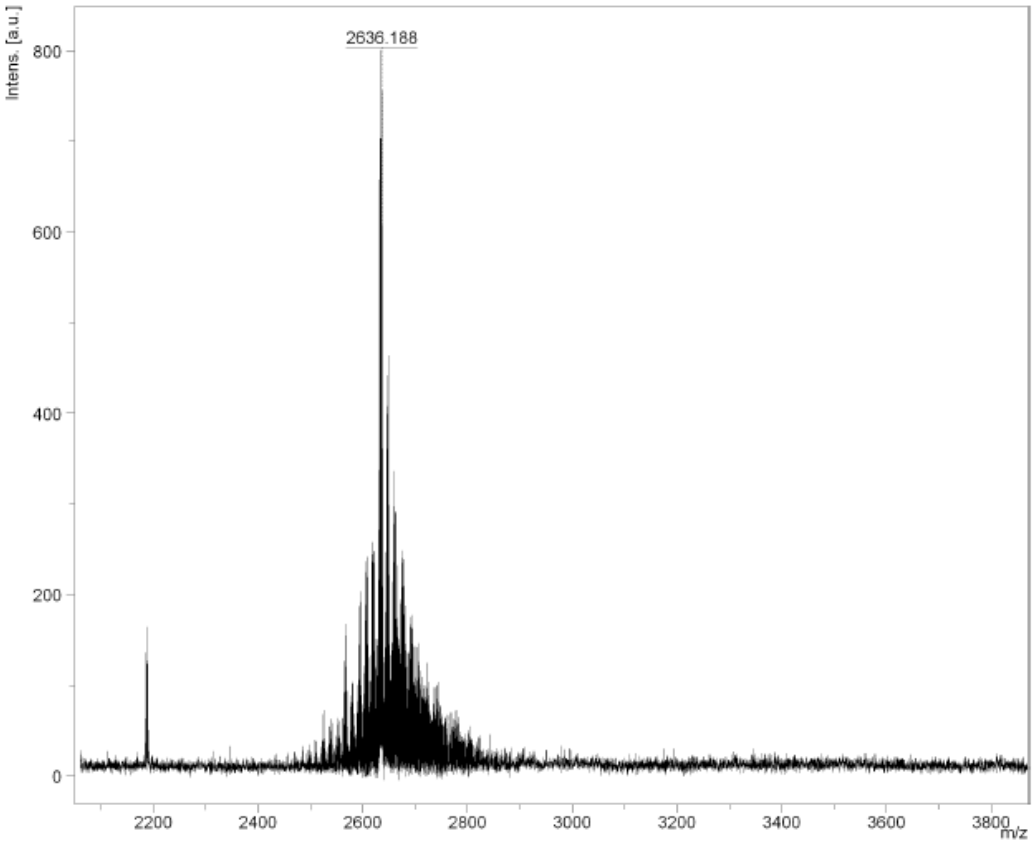

6. References

[1] Becke AD. Density-functional thermochemistry. III. The role of exact exchange, J Chem Phys, 1993; 98: 5648–5652; b) Lee C, Yang W and Parr RG. Development of the Colic-Salvetti correlation-energy formula into a functional of the electron density. Phys Rev B, 1988; 37: 785–789.

[2] Hay PJ and Wadt WRJ. Ab initio effective core potentials for molecular calculations. Potentials for the transition metal atoms Sc to Hg. Chem Phys, 1985; 82: 270–283; b) Wadt WR and Hay PJJ. Ab initio effective core potentials for molecular calculations. Potentials for main group elements Na to Bi. Chem Phys, 1985; 82: 284−298; c) Hay PJ and Wadt WR. Ab initio effective core potentials for molecular calculations. Potentials for K to Au including the outermost core orbitals. J Chem Phys, 1985; 82: 299−310.

[3] Hariharan PC and Pople JA. Accuracy of AH n equilibrium geometries by single determinant molecular orbital theory. Mol Phys, 1974; 27: 209–214.

[4] Lu T and Chen FW. Multiwfn: a multifunctional wavefunction analyzer. J Comput Chem, 2012;

33: 580–592.

[5] Humphrey W, Dalke A and Schulten K. VMD - visual molecular dynamics. J Molec Graphics, 1996; 14: 33–38.

[6] Frisch MJ, Trucks GW, Schlegel HB, Scuseria GE, Robb MA, Cheeseman JR, et al. Gaussian 16, Rev. B.01,Gaussian, Inc., Wallingford CT, 2016.